ERCB/AGS Open File Report 2010-02

ERCB

Mineralogy, Permeametry, Mercury Porosimetry, Pycnometry and Scanning Electron Microscope Imaging of Duvernay and Muskwa Formations in Alberta: Shale Gas Data Release

Energy Resources Conservation Board

AGS
Alberta Geological Survey

ERCB/AGS Open File Report 2010-02

Mineralogy, Permeametry, Mercury Porosimetry, Pycnometry and Scanning Electron Microscope Imaging of Duvernay and Muskwa Formations in Alberta: Shale Gas Data Release

S.D.A. Anderson, C.D. Rokosh, J.G. Pawlowicz
H. Berhane and A. P. Beaton

Energy Resources Conservation Board
Alberta Geological Survey

May 2010

ISBN 978-0-7758-8626-2

Anderson, S.D.A., Rokosh, C.D., Pawlowicz, J.G., Berhane, H. and Beaton, A.P. (2010): Mineralogy, permeametry, mercury porosimetry, pycnometry and scanning electron microscope imaging of the Duvernay and Muskwa formations in Alberta: shale gas data release; Energy Resources Conservation Board, ERCB/AGS Open File Report 2010-02, 67 p.

Published May 2010 by:
Energy Resources Conservation Board
Alberta Geological Survey
4th Floor, Twin Atria Building
4999 – 98th Avenue
Edmonton, Alberta
T6B 2X3
Canada

Tel: 780-422-1927
Fax: 780-422-1918
E-mail: AGS-Info@ercb.ca
Website: www.ags.gov.ab.ca

Contents

Tables

Figures

Acknowledgments

The Alberta Energy Innovation Fund, through the Alberta Department of Energy, has provided partial funding for this project. The authors thank S. Rauschning, K. Henderson and L. Enns from the Alberta Department of Energy for their support of this project. Thanks to Energy Resources Conservation Board Core Research Centre personnel for sampling assistance. Thanks to D-A. Rollings and G. Braybrook for assistance during scanning electron microscope viewing. Thanks to G. Hippolt-Squair of Alberta Geological Survey for her help in putting this report together.

Abstract

This report is a data release of bulk and clay mineralogy, permeametry and mercury porosimetry analyses, helium pycnometry and scanning electron microscope imaging of selected samples from the Duvernay and Muskwa formations generated for the Energy Resources Conservation Board/Alberta Geological Survey project on shale gas resources in Alberta. A few samples were also taken from adjoining formations, such as the Majeau Lake, Beaverhill Lake, Ireton, Fort Simpson, Cooking Lake and Swan Hills. This data release complements other manuscripts and data being released from the same project, as listed in Table 1 of this report.

1 Introduction

The Energy Resources Conservation Board/Alberta Geological Survey (ERCB/AGS) initiated a project in 2007 to evaluate shale gas resources in Alberta, to determine the quantity and spatial extent of these resources. Alberta Geological Survey (AGS) is releasing a series of reports to disseminate data and knowledge from the project. The first formations chosen for evaluation were the Colorado Group (Beaton et al., 2009a; Pawlowicz et al., 2009b), and the Banff and Exshaw formations (Beaton et al., 2009b; Pawlowicz et al., 2009a). These publications are available for download on the AGS website (http://www.ags.gov.ab.ca).

This report disseminates results from bulk and clay mineralogy, permeametry measurements, mercury porosimetry analysis, helium pycnometry and scanning electron microscope (SEM) images from selected samples of the Devonian Duvernay and Muskwa Formations. Table 1 lists all the analyses and associated reports. The data generated from the project will be combined with additional data to map and estimate shale gas resources in the province.

Table 1. Analyses performed on core samples and the organization that performed the analyses as part of the resource evaluation project.

Type of Analysis	Company/Analyst	Notes
Adsorption isotherms	Schlumberger/TerraTek	Beaton et al. (2010a, b)
Mercury porosimetry, envelope and helium pycnometry.	Department of Physics, University of Alberta (D. Schmitt)	Anderson et al. (2010), this report
Permeametry	Department of Earth and Atmospheric Sciences, University of Alberta (M. Gingras)	Anderson et al. (2010), this report
Rock Eval™/TOC	Geological Survey of Canada; Schlumberger/TerraTek	Beaton et al. (2010a, b)
Organic petrography	Geological Survey of Canada (J. Reyes)	Beaton et al. (2010c, d)
Petrographic analysis (thin section)	Alberta Geological Survey	Work in progress
Scanning electron microscope (SEM) with energy-dispersive X-ray (EDX)	Department of Earth and Atmospheric Sciences, University of Alberta (D-A. Rollings, G. Braybrook)	Anderson et al. (2010), this report
X-ray diffraction (bulk and clay mineral)	SGS Mineral Services Ltd. (H. Zhou)	Anderson et al. (2010), this report

2 Sample Location and Description

Figure 1 displays core sample sites associated with the Duvernay and Muskwa formations. Table 2 and Appendix 1 list the locations of the sample sites.

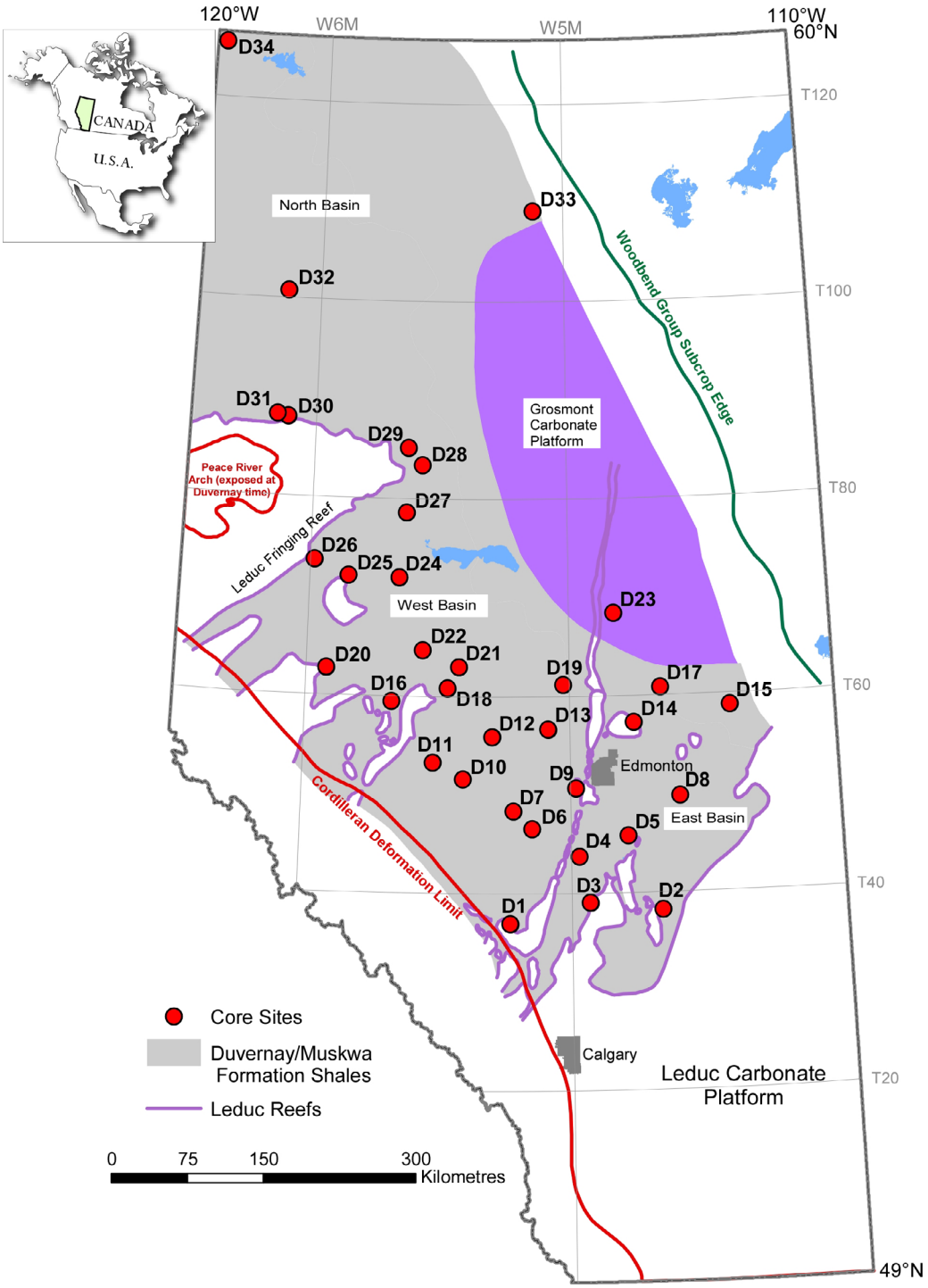

Figure 1. Core sites sampled for the Duvernay and Muskwa formations. See Table 2 and Appendix 1 for a list of all sites and Appendix 2 for the type of analyses run on the samples.

Table 2. Core sample sites in the Duvernay and Muskwa formations. Figure 1 is a map of the sites.

Site No.	Location - UWI	Well Name	Latitude NAD 83	Longitude NAD 83	Year Drilled	No. of Samples
D1	100/06-14-037-07W5/00	CANHUNTER CHEDDARVILLE 6-14-37-7	52.178681	-114.895395	1988	5
D2	100/07-29-038-19W4/00	FCPI ET AL A- 1 STETTLER 7-29-38-19	52.293665	-112.680054	1973	3
D3	100/02-19-039-26W4/00	RIPPER JOFFRE 2-19-39-26	52.364263	-113.729463	1988	4
D4	100/02-08-044-27W4/00	CANETIC RES FBANK 2-8-44-27	52.772473	-113.882727	1955	8
D5	100/10-08-046-22W4/00	IMP HB HAZELWOOD 10-8-46-22	52.954185	-113.157432	1959	6
D6	100/02-06-047-04W5/00	IMP CDN-SUP NORBUCK 2-6-47-4	53.020332	-114.571521	1955	7
D7	100/14-29-048-06W5/00	IMP CDN-SUP PEMBINA 14-29 BR- 48-6	53.176390	-114.845842	1954	7
D8	100/11-11-050-17W4/00	BEAVERHILL LAKE NO. 2 WELL	53.302221	-112.380697	1947	7
D9	100/10-04-051-27W4/00	FORGOTSON- BURK SGSPIKE 10-4-51-27	53.375694	-113.919293	1964	5
D10	100/09-06-052-11W5/00	IMPERIAL CYNTHIA NO. 9-6-52-11	53.463004	-115.601615	1954	14
D11	100/10-30-053-14W5/00	HOME MOBIL PEERS 10-30-53-14	53.608763	-116.049330	1964	14
D12	100/05-17-056-08W5/00	IMPERIAL PADDLE RIVER NO. 1	53.836758	-115.164014	1947	2
D13	100/12-01-057-03W5/00	TEXACO-MCCOLL MAJEAU LAKE #1	53.899127	-114.322013	1948	3
D14	102/10-27-057-21W4/00	ESSO REDWATER 10-27-57-21	53.957625	-113.035417	1981	12
D15	100/10-09-059-11W4/00	SUN IOE LOTTIE 10-9-59-11	54.087511	-111.587683	1963	5
D16	100/10-31-059-18W5/00	TRILOGY KAYBOBS 10-31-59-18	54.146695	-116.686430	1968	5
D17	100/09-09-061-18W4/00	TEXEX ET AL LUCKY 9-9-61-18	54.262405	-112.629101	1951	2
D18	100/15-11-061-13W5/00	WESTGROWTH CARSON 15-11-61-13	54.265106	-115.836890	1980	4
D19	100/10-21-061-01W5/00	IMP WESTLOCK 10-21-61-1	54.292262	-114.086469	1953	4
D20	100/04-11-063-25W5/00	AVONDALE SIMON 4-11-63-25	54.429758	-117.680962	1988	3
D21	100/10-13-063-12W5/00	IMP VIRGINIA HILLS 10-13-63-12	54.452329	-115.674185	1959	4
D22	100/10-05-065-15W5/00	MARATHON VIRGINIA HILLS 10-5-65-15	54.599662	-116.225665	1968	5
D23	100/04-33-068-22W4/00	IMPERIAL DEEP CREEK NO. 4-33-68-22	54.923841	-113.307416	1955	5
D24	100/11-18-072-17W5/00	CEDAR GILWOOD 11-18-72-17	55.238223	-116.607331	1956	2
D25	100/10-24-072-23W5/00	ATLANTIC ETAL WABATANISK 10-24-72-23	55.252641	-117.396100	1965	5
D26	100/16-04-074-26W5/00	DEVON ARL 16B PUSKWASKAU 16-4-74-26	55.386647	-117.930965	2002	8
D27	100/01-01-079-17W5/00	GALLEON DAWSON 1-1-79-17	55.812641	-116.513471	2001	2
D28	100/07-34-083-15W5/00	TOTAL MURPHY SEAL 7-34-83-15	56.235578	-116.276592	1986	3
D29	100/13-20-085-16W5/00	CHEVRON IOE LBUFF 13-20-85-16	56.389314	-116.500762	1972	4
D30	100/11-17-088-03W6/00	PEX ET AL EUREKA 11-17-88-3	56.634242	-118.443537	1983	4
D31	100/02-30-088-04W6/00	TOTAL ATAPCO WORSLEY 2-30-88-4	56.656887	-118.620914	1980	4
D32	100/06-11-101-04W6/00	TEXEX ET AL KEG R 6-11-101-4	57.750185	-118.537350	1957	2
D33	100/14-19-109-03W5/00	IOD IOE T1 FOX LAKE 14-19-109-3	58.485680	-114.495876	1968	6
D34	100/02-04-126-11W6/00	ESSO KAKISA 2-4-126-11	59.913369	-119.842205	1991	8
					Total samples	182

Legend

Column Label	Label Description
Site No.	AGS site location number
Location - UWI	Unique well identifier
Well Name	Name assigned to well when drilling began
Latitude NAD83	Well location - degrees latitude, North American Datum 1983
Longitude NAD83	Well location - degrees longitude, North American Datum 1983
Year Drilled	Year the well was drilled
No. of Samples	Number of samples taken from core

3 Analytical Methods and Results

A total of 182 core samples was collected for analysis. The analyses itemized in Table 1 were performed on selected samples, as indicated in Appendix 2.

3.1 Bulk and Clay Mineralogy

X-ray powder diffraction (XRD) will identify the mineralogy of a sample. Appendices 3 and 4 provide estimates of the weight per cent (wt. %) of each mineral for bulk mineralogy and clay mineralogy, respectively.

X-ray diffraction analysis and interpretation, and X-ray fluorescence spectroscopy (XRF) on core samples were done by SGS Minerals Services Ltd. (http://www.ca.sgs.com/home.htm) using industry-standard techniques.

SGS Minerals uses a Siemens D5000 diffractometer with cobalt radiation and Siemens Search/Match software for peak identification. Mineral proportions are based on relative peak heights and may be strongly influenced by crystallinity, structural group or preferred orientations (H. Zhou, SGS Minerals Services Ltd., pers. comm., 2008; Pecharsky and Zavalij, 2003). The calculation of mineral abundances from both bulk mineral and clay mineral analyses is based on relative peak intensity using the Rietveld reference intensity ratio and is reconciled with a whole-rock analysis by XRF (results provided in Appendix 3b). The detection limit for minerals is approximately 0.5–2.0 wt. % according to SGS, but can be as high as 3–5 wt. % (http://www.xrd.us). Amorphous compounds are not detected by XRD.

Appendix 3 provides bulk mineralogy and X-ray fluorescence spectroscopy data and Appendix 4 gives clay mineralogy. Clay minerals were separated by crushing the sample to 200 mesh and then using a settling column to separate the clay-sized particles. Finally, the sample was centrifuged to remove the liquids before XRD analysis.

3.2 Scanning Electron Microscope and EDX Analysis

The purpose of the scanning electron microscope (SEM) analysis is to characterize the microfabric of the samples, and the morphology, size and distribution of the pores. The SEM can also provide a mineralogical analysis using energy dispersive X-rays (EDX), as well as backscattering images on selected samples. Most samples were analyzed using an SEM fitted with an EDX spectrometer.

The SEM used is a JEOL 6301F (field emission scanning electron microscope) with magnification ranging from 20× to 250 000×. Semiqualitative elemental analysis (EDX) was available via a PGT X-ray analysis system. The lateral resolution and penetration of EDX mineralogical analysis are both about 1 μm.

Appendix 5 provides the SEM images. A brief description accompanies each image; the descriptions are strictly observational. Interpretation of the images, either separately or collectively, in terms of the relationship of microfabric and sedimentology to depositional environment or permeability and porosity will be published later, either in ERCB/AGS open file reports or as journal articles.

3.3 Mercury Porosimetry

Mercury porosimetry is a technique to quantify intrusion pore diameter, size range of diameters, pore volume and pore surface area of the samples (Webb and Orr, 1997). Porosimeter work was done at the University of Alberta. All samples were put under vacuum in a cold oven for degassing prior to analysis. Mercury was introduced into the sample and the volume of mercury forced into pore space in the sample used to calculate pore volume for the sample. The graphs in Appendix 6 show incremental intrusion versus pore diameter, which is meant to portray the concentration of pore throat sizes in the sample, and

log differential intrusion versus pore diameter, in which equal peak areas represent equal volume of pore sizes (Webb and Orr, 1997).

The sample size is rather small (tens of grams), so the data do not necessarily represent regional pore throat sizes of the formation. The variables graphed are two of a number of data columns available for analysis, including cumulative intrusion, incremental intrusion, differential intrusion, log differential intrusion, cumulative pore volume, cumulative pore area and fractal dimensions. The definition and derivation of these values are well explained by Webb and Orr (1997). The lab also calculated a number of other variables using the original measured data, including bulk density, skeletal density, sample porosity, permeability and surface area.

The graphs in Appendix 6 express pore diameter in terms of equivalent spherical diameter (Webb and Orr, 1997). If the pore throat is smaller than the diameter of the pore, then the mercury must first intrude through the smaller pore throat to enter the larger pore; hence, the 'pore diameter' reflected on the graphs is often referred to as the 'pore throat' diameter. All incremental intrusion values that are negative are assigned a value of zero. The graphs include two grain-size scales: the International Union of Pure and Applied Chemistry (IUPAC) pore classification (Rouquerol et al., 1994) used by some authors (e.g., Ross and Bustin, 2008) and the more traditional grain-size scale of Wentworth (1922) with a 3.9 μm clay-silt boundary. The first two sample points at the highest pore diameter generally exhibit a peak that is an artifact of the sample process and is not likely a real pore diameter. A number of samples underwent repeat analysis to test for precision; the samples used were fresh and were taken at the same depth.

The data in this study were generated using the Washburn equation ($D = -4\gamma\cos\theta/P$), where γ is the surface tension, θ is the assumed contact angle of mercury, P is the applied pressure and D is the equivalent pore diameter. The term 'equivalent' is used because the equation assumes all pores are the equivalent shape of a cylinder; in reality, this is not the case. The surface tension (485 dynes/cm), contact angle (130°) and equilibration time (10 seconds) between successive increases in pressure used in the procedure are all recommended by the manufacturer.

If pores are assumed to be dominated by 'slit-like' openings, as in clay-dominated sediment, then the data may be recalculated using $W = -2\gamma\cos\theta/P$, where W is the width between plates (Webb and Orr 1997). However, the samples in this study are dominantly silt-rich shale/mudstone or shaly siltstone, so we are comfortable using the Washburn equation as a starting point of analysis.

A summary of the procedure can be found in Webb and Orr (1997) and D'Souzae and More (2008).

3.4 Permeametry

Spot permeametry analysis (Gingras et al., 2004) was carried out at the University of Alberta on a portable probe permeameter (CoreLabs Model PP-250), with nitrogen and air as the pore fluids. Note that the diameter of a nitrogen molecule is about 0.15 nm (1.5 angstroms), while the diameter of a methane molecule is about 0.4 nm (4.0 angstroms). Each sample is generally tested three or more times in one spot. Horizontal and vertical permeability were tested in some samples. Appendix 7 provides the data for each sample.

3.5 Helium Pycnometry

Helium pycnometry measures grain density (often called skeletal density, apparent density, true density or absolute density), which is the density of a substance excluding pores large enough for helium to penetrate (Webb and Orr, 1997). Hence, pores that are not connected are not accounted for in this process. Appendix 8 presents the helium pycnometry data.

4 References

Anderson, S.D.A., Rokosh, C.D., Pawlowicz, J.G., Berhane, H. and Beaton, A.P. (2010): Mineralogy, permeametry, mercury porosimetry, pycnometry and scanning electron microscope imaging of the Montney Formation in Alberta: shale gas data release; Energy Resources Conservation Board, ERCB/AGS Open File Report 2010-03, 61 p., URL <http://www.ags.gov.ab.ca/publications/abstracts/OFR_2010_03.html> [April 16, 2010].

Beaton, A.P., Pawlowicz, J.G., Anderson, S.D.A., Berhane, H. and Rokosh, C.D. (2010a): Organic petrography of the Duvernay and Muskwa Formations in Alberta: shale gas data release; Energy Resources Conservation Board, ERCB/AGS Open File Report 2010-06, 20 p., URL <http://www.ags.gov.ab.ca/publications/abstracts/OFR_2010_06.html> [April 16, 2010].

Beaton, A.P., Pawlowicz, J.G., Anderson, S.D.A., Berhane, H. and Rokosh, C.D. (2010b): Organic petrography of the Montney Formation in Alberta: shale gas data release; Energy Resources Conservation Board, ERCB/AGS Open File Report 2010-07, 24 p., URL <http://www.ags.gov.ab.ca/publications/abstracts/OFR_2010_07.html> [April 16, 2010].

Beaton, A.P., Pawlowicz, J.G., Anderson, S.D.A. and Rokosh, C.D. (2009a): Rock Eval™, total organic carbon, isotherms and organic petrography of the Colorado Group: shale gas data release; Energy Resources Conservation Board, ERCB/AGS Open File Report 2008-11, 88 p., URL <http://www.ags.gov.ab.ca/publications/abstracts/OFR_2008_11.html> [April 16, 2010].

Beaton, A.P., Pawlowicz, J.G., Anderson, S.D.A. and Rokosh, C.D. (2009b): Rock Eval™, total organic carbon, isotherms and organic petrography of the Banff and Exshaw formations: shale gas data release; Energy Resources Conservation Board, ERCB/AGS Open File Report 2008-12, 65 p., URL <http://www.ags.gov.ab.ca/publications/abstracts/OFR_2008_12.html> [April 16, 2010].

Beaton, A.P., Pawlowicz, J.G., Anderson, S.D.A., Berhane, H. and Rokosh, C.D. (2010c): Rock Eval™, total organic carbon and adsorption isotherms of the Montney Formation in Alberta: shale gas data release; Energy Resources Conservation Board, ERCB/AGS Open File Report 2010-05, 30 p., URL <http://www.ags.gov.ab.ca/publications/abstracts/OFR_2010_05.html> [April 16, 2010].

Beaton, A.P., Pawlowicz, J.G., Anderson, S.D.A., Berhane, H. and Rokosh, C.D. (2010d): Rock Eval™, total organic carbon and adsorption isotherms of the Duvernay and Muskwa formations in Alberta: shale gas data release; Energy Resources Conservation Board, ERCB/AGS Open File Report 2010-04, 32 p., URL <http://www.ags.gov.ab.ca/publications/abstracts/OFR_2010_04.html> [April 2010].

D'Souzae, J.I. and More, H.N. (2008): Pharmaceutical powder material contains void volume of empty space, distributed within the solid mass in the form of pores, cavities, and cracks of various shapes and sizes; Pharminfo.net, URL <http://www.pharmainfo.net/reviews/mercury-intrusion-porosimetry-tool-pharmaceutical-particle-characterization> [January 13, 2010].

Gingras, M.K., Mendoza, C.A. and Pemberton, S.G. (2004): Fossilized worm burrows influence the resource quality of porous media; AAPG Bulletin, v. 88, no. 7, p. 875–883.

Pawlowicz, J.G., Anderson, S.D.A., Rokosh, C.D. and Beaton, A.P. (2009a): Mineralogy, permeametry, mercury porosimetry and scanning electron microscope imaging of the Banff and Exshaw formations: shale gas data release; Energy Resources Conservation Board, ERCB/AGS Open File Report 2008-13, 59 p., URL <http://www.ags.gov.ab.ca/publications/abstracts/OFR_2008_13.html> [April 16, 2010].

Pawlowicz, J.G., Anderson, S.D.A., Rokosh, C.D. and Beaton, A.P. (2009b): Mineralogy, permeametry, mercury porosimetry and scanning electron microscope imaging of the Colorado Group: shale gas data release; Energy Resources Conservation Board, ERCB/AGS Open File Report 2008-14, 92 p., URL <http://www.ags.gov.ab.ca/publications/abstracts/OFR_2008_14.html> [April 16, 2010].

Pecharsky, V.K. and Zavalij, P.Y. (2003): Fundamentals of powder diffraction and structural characterization of minerals; Kluwer Academic Publishers, New York, 713 p.

Ross, D.J.K. and Bustin, R.M. (2008): The importance of shale composition and pore structure upon gas storage potential of shale gas reservoirs; Marine and Petroleum Geology, v. 26, p. 916–927.

Rouquerol, J., Avnir, D., Fairbridge, C.W., Everett, D.H., Haynes, J.H., Pernicone, N., Ramsay, J.D.F., Sing, K.S.W. and Unger, K. (1994): Recommendations for the characterization of porous solids, International Union of Pure and Applied Chemistry; Pure and Applied Chemistry, v. 68, p. 1739–1758.

Webb, P.A. and Orr, C. (1997): Analytical methods in fine particle technology; Micromeritics Instrument Corporation Publishers, Norcross, Georgia.

Wentworth, C. K. (1922): A scale of grade and class terms for clastic sediments; Journal of Geology, v. 30, p. 377–392.

Appendices

Appendix 1 – Duvernay and Muskwa Formations Core Sample Location, Depth and Lithology

Legend

Column Label	Label Description
Sample No.	AGS sample number
Site No.	AGS site location number
Location - UWI	Well location - unique well identifier
Sample Depth (metres)	Depth of core sample in metres (measured from core)
Lithology	Brief lithological description of sample
Formation/Group	Geological formation or group at depth of sample

Sample No.	Site No.	Location - UWI	Sample Depth (Metres)	Lithology	Formation/Group
8127	D30	100/11-17-088-03W6/00	2317.5	shale	Muskwa
8128	D30	100/11-17-088-03W6/00	2319.3	shale	Muskwa
8129	D30	100/11-17-088-03W6/00	2324.4	shale	Muskwa
8130	D30	100/11-17-088-03W6/00	2339.0	carbonate mudstone	Beaverhill Lake
8133	D8	100/11-11-050-17W4/00	1135.1	shale	Ireton
8134	D8	100/11-11-050-17W4/00	1163.1	shale	Ireton
8135	D8	100/11-11-050-17W4/00	1182.6	shale	Duvernay
8136	D8	100/11-11-050-17W4/00	1190.2	shale	Duvernay
8137	D8	100/11-11-050-17W4/00	1204.3	shale	Duvernay
8138	D8	100/11-11-050-17W4/00	1220.4	shale	Duvernay
8139	D8	100/11-11-050-17W4/00	1270.7	carbonate mudstone	Cooking Lake
8140	D25	100/10-24-072-23W5/00	2821.2	shale	Duvernay
8141	D25	100/10-24-072-23W5/00	2825.5	shale	Duvernay
8142	D25	100/10-24-072-23W5/00	2832.2	shale	Duvernay
8143	D25	100/10-24-072-23W5/00	2837.7	shale	Duvernay
8144	D25	100/10-24-072-23W5/00	2844.1	shale	Beaverhill Lake
8145	D33	100/14-19-109-03W5/00	372.0	chalk	Ireton
8146	D33	100/14-19-109-03W5/00	374.0	shale	Ireton
8147	D33	100/14-19-109-03W5/00	410.0	shale	Ireton
8148	D33	100/14-19-109-03W5/00	456.0	shale	Ireton
8149	D33	100/14-19-109-03W5/00	503.0	shale	Ireton
8150	D33	100/14-19-109-03W5/00	553.0	shale	Ireton
8451	D23	100/04-33-068-22W4/00	1030.1	carbonate mudstone	Duvernay
8452	D23	100/04-33-068-22W4/00	1043.6	carbonate mudstone	Duvernay
8453	D23	100/04-33-068-22W4/00	1052.8	carbonate mudstone	Duvernay
8454	D23	100/04-33-068-22W4/00	1054.6	carbonate mudstone	Duvernay
8455	D23	100/04-33-068-22W4/00	1061.6	dolostone	Cooking Lake
8456	D12	100/05-17-056-08W5/00	2358.8	shale	Duvernay
8457	D12	100/05-17-056-08W5/00	2386.9	shale	Duvernay
8458	D15	100/10-09-059-11W4/00	774.3	shale	Duvernay
8459	D15	100/10-09-059-11W4/00	786.1	carbonate mudstone	Duvernay
8460	D15	100/10-09-059-11W4/00	793.7	carbonate mudstone	Duvernay
8461	D15	100/10-09-059-11W4/00	797.7	carbonate mudstone	Duvernay
8462	D15	100/10-09-059-11W4/00	798.6	carbonate mudstone	Duvernay
8463	D14	102/10-27-057-21W4/00	1134.7	carbonate mudstone	Duvernay
8464	D14	102/10-27-057-21W4/00	1136.8	carbonate mudstone	Duvernay
8465	D14	102/10-27-057-21W4/00	1139.4	carbonate mudstone	Duvernay
8466	D14	102/10-27-057-21W4/00	1141.4	carbonate mudstone	Duvernay
8467	D14	102/10-27-057-21W4/00	1149.5	carbonate mudstone	Duvernay
8468	D14	102/10-27-057-21W4/00	1149.8	carbonate mudstone	Duvernay
8469	D14	102/10-27-057-21W4/00	1151.5	carbonate mudstone	Duvernay
8470	D14	102/10-27-057-21W4/00	1153.7	carbonate mudstone	Duvernay
8471	D14	102/10-27-057-21W4/00	1157.4	carbonate mudstone	Duvernay
8472	D14	102/10-27-057-21W4/00	1161.3	carbonate mudstone	Duvernay
8473	D14	102/10-27-057-21W4/00	1162.2	carbonate mudstone	Duvernay
8474	D14	102/10-27-057-21W4/00	1162.6	carbonate mudstone	Duvernay
8476	D12	100/05-17-056-08W5/00	2386.9	duplicate of sample 8457	Duvernay
8479	D21	100/10-13-063-12W5/00	2618.4	shale	Majeau Lake
8480	D21	100/10-13-063-12W5/00	2621.9	shale	Majeau Lake
8481	D21	100/10-13-063-12W5/00	2625.5	shale	Majeau Lake
8482	D21	100/10-13-063-12W5/00	2632.6	carbonate mudstone	Beaverhill Lake
8483	D9	100/10-04-051-27W4/00	1934.9	shale	Duvernay
8484	D9	100/10-04-051-27W4/00	1938.2	shale	Duvernay

Sample No.	Site No.	Location - UWI	Sample Depth (Metres)	Lithology	Formation/Group
8485	D9	100/10-04-051-27W4/00	1941.3	shale	Duvernay
8486	D9	100/10-04-051-27W4/00	1944.3	shale	Duvernay
8487	D9	100/10-04-051-27W4/00	1947.4	shale	Duvernay
8488	D7	100/14-29-048-06W5/00	2638.0	carbonate mudstone	Duvernay
8489	D7	100/14-29-048-06W5/00	2643.2	carbonate mudstone	Duvernay
8490	D7	100/14-29-048-06W5/00	2648.7	shale	Duvernay
8491	D7	100/14-29-048-06W5/00	2652.8	shale	Duvernay
8492	D7	100/14-29-048-06W5/00	2655.7	shale	Duvernay
8493	D7	100/14-29-048-06W5/00	2656.5	shale	Duvernay
8494	D7	100/14-29-048-06W5/00	2660.0	carbonate mudstone	Duvernay
8495	D18	100/15-11-061-13W5/00	2542.8	shale	Majeau Lake
8496	D18	100/15-11-061-13W5/00	2545.1	shale	Majeau Lake
8497	D18	100/15-11-061-13W5/00	2549.7	carbonate mudstone	Majeau Lake
8498	D18	100/15-11-061-13W5/00	2551.8	carbonate mudstone	Beaverhill Lake
8499	D32	100/06-11-101-04W6/00	1651.4	shale	Muskwa
8500	D32	100/06-11-101-04W6/00	1652.3	shale	Muskwa
8978	D3	100/02-19-039-26W4/00	2278.2	carbonate mudstone	Duvernay
8979	D3	100/02-19-039-26W4/00	2280.4	carbonate mudstone	Duvernay
8980	D3	100/02-19-039-26W4/00	2285.4	carbonate mudstone	Duvernay
8981	D3	100/02-19-039-26W4/00	2290.5	carbonate mudstone	Duvernay
8982	D2	100/07-29-038-19W4/00	1773.3	carbonate mudstone	Duvernay
8983	D2	100/07-29-038-19W4/00	1775.9	shale	Duvernay
8984	D2	100/07-29-038-19W4/00	1786.1	carbonate mudstone	Duvernay
8985	D27	100/01-01-079-17W5/00	2217.0	carbonate mudstone	Beaverhill Lake
8986	D27	100/01-01-079-17W5/00	2224.8	carbonate mudstone	Beaverhill Lake
8987	D29	100/13-20-085-16W5/00	1684.9	carbonate mudstone	Ireton
8988	D29	100/13-20-085-16W5/00	1689.5	carbonate mudstone	Ireton
8989	D29	100/13-20-085-16W5/00	1704.1	shale	Duvernay
8990	D28	100/07-34-083-15W5/00	1773.0	shale	Ireton
8991	D28	100/07-34-083-15W5/00	1777.7	shale	Duvernay
8992	D28	100/07-34-083-15W5/00	1781.2	gneiss	PC
8993	D29	100/13-20-085-16W5/00	1704.7	shale	Duvernay
8994	D31	100/02-30-088-04W6/00	2392.0	shale	Ireton
8995	D31	100/02-30-088-04W6/00	2401.2	shale	Muskwa
8996	D31	100/02-30-088-04W6/00	2405.2	shale	Muskwa
8997	D31	100/02-30-088-04W6/00	2413.4	carbonate mudstone	Muskwa
8998	D4	100/02-08-044-27W4/00	2206.8	shale	Ireton
8999	D4	100/02-08-044-27W4/00	2231.4	shale	Ireton
9000	D4	100/02-08-044-27W4/00	2235.3	carbonate mudstone	Duvernay
9201	D20	100/04-11-063-25W5/00	3578.5	carbonate mudstone	Beaverhill Lake
9202	D10	100/09-06-052-11W5/00	3013.9	shale	Duvernay
9203	D10	100/09-06-052-11W5/00	3015.2	shale	Duvernay
9204	D10	100/09-06-052-11W5/00	3015.7	shale	Duvernay
9205	D10	100/09-06-052-11W5/00	3016.3	shale	Duvernay
9206	D10	100/09-06-052-11W5/00	3017.1	shale	Duvernay
9207	D10	100/09-06-052-11W5/00	3018.3	shale	Duvernay
9208	D10	100/09-06-052-11W5/00	3018.7	shale	Duvernay
9209	D10	100/09-06-052-11W5/00	3019.3	shale	Duvernay
9210	D10	100/09-06-052-11W5/00	3020.1	shale	Duvernay
9211	D10	100/09-06-052-11W5/00	3020.9	shale	Duvernay
9212	D10	100/09-06-052-11W5/00	3021.8	carbonate mudstone	Duvernay
9213	D10	100/09-06-052-11W5/00	3023.3	carbonate mudstone	Duvernay
9214	D10	100/09-06-052-11W5/00	3024.7	carbonate mudstone	Duvernay
9215	D10	100/09-06-052-11W5/00	3025.7	carbonate mudstone	Duvernay
9216	D16	100/10-31-059-18W5/00	3196.7	carbonate mudstone	Beaverhill Lake
9217	D16	100/10-31-059-18W5/00	3201.6	carbonate mudstone	Swan Hills
9218	D16	100/10-31-059-18W5/00	3205.3	carbonate mudstone	Swan Hills
9219	D16	100/10-31-059-18W5/00	3210.5	carbonate mudstone	Swan Hills
9220	D16	100/10-31-059-18W5/00	3216.4	carbonate mudstone	Swan Hills
9221	D13	100/12-01-057-03W5/00	1823.8	carbonate mudstone	Duvernay
9222	D13	100/12-01-057-03W5/00	1825.3	shale	Duvernay
9223	D13	100/12-01-057-03W5/00	1829.4	carbonate mudstone	Duvernay

Sample No.	Site No.	Location - UWI	Sample Depth (Metres)	Lithology	Formation/Group
9224	D22	100/10-05-065-15W5/00	2747.8	shale	Duvernay
9225	D22	100/10-05-065-15W5/00	2749.6	shale	Duvernay
9226	D22	100/10-05-065-15W5/00	2752.0	shale	Duvernay
9227	D22	100/10-05-065-15W5/00	2757.7	shale	Duvernay
9228	D22	100/10-05-065-15W5/00	2760.9	shale	Duvernay
9229	D19	100/10-21-061-01W5/00	1461.5	carbonate mudstone	Duvernay
9230	D19	100/10-21-061-01W5/00	1464.9	carbonate mudstone	Duvernay
9231	D19	100/10-21-061-01W5/00	1469.4	carbonate mudstone	Duvernay
9232	D19	100/10-21-061-01W5/00	1473.1	shale	Duvernay
9233	D17	100/09-09-061-18W4/00	897.3	carbonate mudstone	Duvernay
9234	D17	100/09-09-061-18W4/00	957.7	carbonate mudstone	Duvernay
9235	D1	100/06-14-037-07W5/00	3640.3	carbonate mudstone	Duvernay
9236	D1	100/06-14-037-07W5/00	3642.6	carbonate mudstone	Duvernay
9237	D1	100/06-14-037-07W5/00	3649.1	shale	Duvernay
9238	D1	100/06-14-037-07W5/00	3649.7	shale	Duvernay
9239	D1	100/06-14-037-07W5/00	3653.1	shale	Duvernay
9240	D24	100/11-18-072-17W5/00	2362.8	shale	Duvernay
9241	D24	100/11-18-072-17W5/00	2364.9	shale	Duvernay
9242	D4	100/02-08-044-27W4/00	2206.8	duplicate of sample 8998	Ireton
9243	D11	100/10-30-053-14W5/00	3177.4	duplicate of sample 9389	Majeau Lake
9244	D10	100/09-06-052-11W5/00	3015.7	duplicate of sample 9204	Duvernay
9245	D24	100/11-18-072-17W5/00	2362.8	duplicate of sample 9240	Duvernay
9246	D25	100/10-24-072-23W5/00	2757.7	duplicate of sample 9227	Duvernay
9261	D25	100/10-24-072-23W5/00	2821.2 - 2832.2	combined sample # 8140, 8142	Duvernay
9262	D21	100/10-13-063-12W5/00	2621.9 - 2625.5	combined sample # 8480, 8481	Majeau Lake
9263	D11	100/10-30-053-14W5/00	3168.9 - 3169.8	combined sample # 9387, 9388	Majeau Lake
9264	D10	100/09-06-052-11W5/00	3018.3 - 3020.1	combined sample # 9207, 9208, 9209, 9210	Duvernay
9265	D26	100/16-04-074-26W5/00	2940 - 2941.8	combined sample # 9351, 9352	Duvernay
9266	D32	100/06-11-101-04W6/00	1651.4 - 1652.3	combined sample # 8499, 8500	Muskwa
9267	D24	100/11-18-072-17W5/00	2362.8 - 2364.9	combined sample # 9240, 9241	Duvernay
9268	D19	100/10-21-061-01W5/00	1461.5 - 1464.8	combined sample # 9229, 9230	Duvernay
9351	D26	100/16-04-074-26W5/00	2940.0	shale	Duvernay
9352	D26	100/16-04-074-26W5/00	2941.8	shale	Duvernay
9353	D26	100/16-04-074-26W5/00	2942.6	shale	Duvernay
9354	D26	100/16-04-074-26W5/00	2943.8	shale	Majeau Lake
9355	D26	100/16-04-074-26W5/00	2946.3	shale	Beaverhill Lake
9356	D26	100/16-04-074-26W5/00	2948.3	shale	Beaverhill Lake
9357	D26	100/16-04-074-26W5/00	2950.0	carbonate mudstone	Beaverhill Lake
9358	D26	100/16-04-074-26W5/00	2956.4	carbonate mudstone	Beaverhill Lake
9359	D6	100/02-06-047-04W5/00	2628.9	shale	Duvernay
9360	D6	100/02-06-047-04W5/00	2635.3	shale	Duvernay
9361	D6	100/02-06-047-04W5/00	2638.3	shale	Duvernay
9362	D6	100/02-06-047-04W5/00	2639.6	shale	Duvernay
9363	D6	100/02-06-047-04W5/00	2642.6	shale	Duvernay
9364	D6	100/02-06-047-04W5/00	2644.7	shale	Duvernay
9365	D6	100/02-06-047-04W5/00	2647.8	shale	Duvernay
9366	D34	100/02-04-126-11W6/00	1515.0	shale	Muskwa
9367	D34	100/02-04-126-11W6/00	1517.4	shale	Muskwa
9368	D34	100/02-04-126-11W6/00	1519.8	shale	Muskwa
9369	D34	100/02-04-126-11W6/00	1521.2	shale	Muskwa
9370	D34	100/02-04-126-11W6/00	1523.6	shale	Muskwa
9371	D34	100/02-04-126-11W6/00	1526.0	shale	Muskwa
9372	D34	100/02-04-126-11W6/00	1528.4	shale	Muskwa
9373	D34	100/02-04-126-11W6/00	1533.0	shale	Muskwa
9374	D4	100/02-08-044-27W4/00	2243.3	shale	Duvernay
9375	D4	100/02-08-044-27W4/00	2245.8	shale	Duvernay
9376	D4	100/02-08-044-27W4/00	2253.1	shale	Duvernay
9377	D4	100/02-08-044-27W4/00	2256.4	carbonate mudstone	Duvernay
9378	D4	100/02-08-044-27W4/00	2274.7	carbonate mudstone	Cooking Lake
9379	D5	100/10-08-046-22W4/00	1700.8	carbonate mudstone	Duvernay
9380	D5	100/10-08-046-22W4/00	1708.6	carbonate mudstone	Duvernay
9381	D5	100/10-08-046-22W4/00	1721.1	carbonate mudstone	Duvernay

Sample No.	Site No.	Location - UWI	Sample Depth (Metres)	Lithology	Formation/Group
9382	D5	100/10-08-046-22W4/00	1722.1	carbonate mudstone	Duvernay
9383	D5	100/10-08-046-22W4/00	1728.5	carbonate mudstone	Duvernay
9384	D5	100/10-08-046-22W4/00	1741.2	carbonate mudstone	Cooking Lake
9385	D11	100/10-30-053-14W5/00	3167.2	shale	Majeau Lake
9386	D11	100/10-30-053-14W5/00	3167.9	shale	Majeau Lake
9387	D11	100/10-30-053-14W5/00	3168.9	shale	Majeau Lake
9388	D11	100/10-30-053-14W5/00	3169.8	shale	Majeau Lake
9389	D11	100/10-30-053-14W5/00	3170.5	shale	Majeau Lake
9390	D11	100/10-30-053-14W5/00	3171.4	shale	Majeau Lake
9391	D11	100/10-30-053-14W5/00	3172.4	shale	Majeau Lake
9392	D11	100/10-30-053-14W5/00	3172.8	shale	Majeau Lake
9393	D11	100/10-30-053-14W5/00	3173.4	shale	Majeau Lake
9394	D11	100/10-30-053-14W5/00	3173.9	shale	Majeau Lake
9395	D11	100/10-30-053-14W5/00	3175.4	shale	Majeau Lake
9396	D11	100/10-30-053-14W5/00	3176.0	shale	Majeau Lake
9397	D11	100/10-30-053-14W5/00	3176.6	shale	Majeau Lake
9398	D11	100/10-30-053-14W5/00	3177.4	shale	Majeau Lake
9399	D20	100/04-11-063-25W5/00	3576.3	shale	Ireton
9400	D20	100/04-11-063-25W5/00	3576.8	shale	Ireton

Appendix 2 – Duvernay and Muskwa Formations Samples Analyzed

Legend
Y = Sample data presented in this report
x = Sample data presented in other Alberta Geological Survey reports (see Table 1 for details)
z = Data are being analyzed and will be distributed in a future report
Analyses presented in this report

Column Label	Label Description
Sample No.	AGS sample number
Site No.	Site location number
Rock Eval™ TOC	Rock Eval™ pyrolysis is used to identify the type and maturity of organic matter and to detect petroleum potential in sediments. Total Organic Carbon is a measure of the amount of organic carbon in the sediment (in weight per cent).
XRD-Bulk	X-Ray diffraction analysis of whole rock mineralogy
XRD-Clay	X-Ray diffraction analysis of clay mineralogy
Organic Pet.	Petrographic imaging and description of organic macerals
Thin Section	Thin section of sample
Adsorption Isotherm	Gas adsorption analysis to determine gas-holding capacity of sample
SEM	Scanning electron microscope
Mini-perm	Analysis to determine permeability
Porosimetry	Analysis to determine pore-throat size
Pycnometry	Analysis to determine grain density
Texture with Clay Mineralogy	Determination of sand, silt and clay size distribution in weight per cent with clay mineralogy on clay separates.

Sample No.	Site No.	Rock Eval™ TOC	XRD-Bulk	XRD-Clay	Organic Pet.	Thin Section	Adsorption Isotherm	SEM	Mini-perm	Porosimetry	Pycnometry	Texture with Clay Mineralogy
8127	D30	x			z							
8128	D30	x				z						
8129	D30	x										
8130	D30	x										
8133	D8	x										
8134	D8	x										
8135	D8	x	Y									
8136	D8	x			z							
8137	D8	x										
8138	D8	x										
8139	D8	x										
8140	D25	x			z							
8141	D25	x										z
8142	D25	x			z							
8143	D25	x										
8144	D25	x										
8145	D33	x										
8146	D33											
8147	D33	x										
8148	D33											
8149	D33	x			z							
8150	D33											
8451	D23	x										
8452	D23	x										
8453	D23	x										
8454	D23	x			z	z						
8455	D23	x										
8456	D12	x	Y		z							
8457	D12	x										
8458	D15	x										
8459	D15	x										
8460	D15	x										
8461	D15	x	Y		z	z						
8462	D15	x										
8463	D14	x										
8464	D14	x			z							
8465	D14	x										
8466	D14	x										
8467	D14	x			z							
8468	D14	x										
8469	D14	x										
8470	D14	x			z							
8471	D14	x										
8472	D14	x										
8473	D14	x										
8474	D14	x			z							
8476	D12	x										
8479	D21	x						Y		Y	Y	
8480	D21	x	Y									
8481	D21	x			z	z						
8482	D21	x			z							
8483	D9	x			z							
8484	D9	x										z
8485	D9	x			z							
8486	D9	x										
8487	D9	x										
8488	D7											
8489	D7	x										
8490	D7	x			z							z
8491	D7	x										
8492	D7	x			z	z						
8493	D7	x								z	Y	
8494	D7	x										
8495	D18	x										
8496	D18	x										
8497	D18	x			z							
8498	D18	x										
8499	D32	x			z							
8500	D32	x										
8978	D3	x										
8979	D3	x			z							
8980	D3	x										
8981	D3	x										
8982	D2	x										
8983	D2	x			z							z
8984	D2	x										
8985	D27	x										
8986	D27	x										
8987	D29											
8988	D29	x										
8989	D29	x			z							
8990	D28	x										

Sample No.	Site No.	Rock Eval™ TOC	XRD-Bulk	XRD-Clay	Organic Pet.	Thin Section	Adsorption Isotherm	SEM	Mini-perm	Porosimetry	Pycnometry	Texture with Clay Mineralogy
8991	D28	x										
8992	D28											
8993	D29	x			z							
8994	D31	x										
8995	D31	x				z	x			Y	Y	
8996	D31	x	Y	Y								
8997	D31	x			z							
8998	D4	x										
8999	D4	x										
9000	D4	x			z							
9201	D20	x										
9202	D10	x			z							
9203	D10	x										
9204	D10	x										
9205	D10	x	Y	Y								
9206	D10	x										z
9207	D10	x										
9208	D10	x						Y	Y	z	Y	
9209	D10	x										
9210	D10	x				z						
9211	D10	x										
9212	D10	x										
9213	D10											
9214	D10	x										
9215	D10											
9216	D16	x										
9217	D16											
9218	D16	x										
9219	D16											
9220	D16	x										
9221	D13	x										
9222	D13	x			z							
9223	D13	x										
9224	D22	x										
9225	D22	x										
9226	D22	x				z						
9227	D22	x										
9228	D22	x	Y	Y	z					z	Y	
9229	D19	x										
9230	D19	x										
9231	D19	x										
9232	D19	x			z			Y				
9233	D17	x			z							
9234	D17	x										
9235	D1	x	Y	Y								
9236	D1	x										
9237	D1	x			z				Y			
9238	D1	x				z		Y		Y	Y	
9239	D1	x										
9240	D24	x			z							
9241	D24	x										
9242	D4	x										
9243	D11	x										
9244	D10	x			z							
9245	D24	x										
9246	D25	x			z							
9261	D25	x					x					
9262	D21	x					x					
9263	D11	x					x					
9264	D10	x					x					
9265	D26	x					x					
9266	D32		Y	Y								
9267	D24		Y	Y								
9268	D19		Y	Y								
9351	D26	x			z							
9352	D26	x										
9353	D26	x										
9354	D26	x										
9355	D26	x										
9356	D26	x										
9357	D26	x										
9358	D26											
9359	D6	x										
9360	D6	x										
9361	D6	x										
9362	D6	x	Y	Y	z	z						
9363	D6	x										
9364	D6	x					x					
9365	D6	x						Y	Y	z	Y	
9366	D34	x										z
9367	D34	x				z						
9368	D34	x			z							
9369	D34	x										
9370	D34	x						Y		Y	Y	
9371	D34	x										
9372	D34	x	Y	Y								
9373	D34	x					x					
9374	D4	x										
9375	D4	x	Y	Y								
9376	D4	x										
9377	D4	x			z							
9378	D4	x			z							
9379	D5	x										
9380	D5	x	Y	Y			x					
9381	D5	x										
9382	D5	x			z							
9383	D5	x										
9384	D5	x										
9385	D11	x										
9386	D11	x	Y	Y				Y	Y	z	Y	
9387	D11	x										
9388	D11	x										
9389	D11	x										
9390	D11	x										
9391	D11	x										
9392	D11	x				z						

Sample No.	Site No.	Rock Eval™ TOC	XRD-Bulk	XRD-Clay	Organic Pet.	Thin Section	Adsorption Isotherm	SEM	Mini-perm	Porosimetry	Pycnometry	Texture with Clay Mineralogy
9393	D11	x										
9394	D11	x										
9395	D11	x										
9396	D11	x										
9397	D11	x										
9398	D11	x										
9399	D20	x			z							
9400	D20	x										

Appendix 3 – Duvernay and Muskwa Formations Bulk Sample Mineralogy (XRD)

Appendix 3a – Bulk X-Ray Diffraction

Sample No.	Site No.	Quartz	Feldspars			Pyrite	Hem.	Clay Minerals							Carbonates				Sulphate	FlAp.	Brkt.	Total
			Albite	Micro.	Ortho.			Musc.	Bio.	Paly.	Kaol.	Illite	Mont.	ClCh.	Calcite	Dolo.	Ank.	Rhod.	Gyp.			
8135	D8	12.3	2.5		2.9	3.5		15.4						2.9	54.5	2.1	3.0	0.1		0.7	0.3	100.2
8456	D12	46.5	3.5		3.5	2.5	0.5	14.4			3.9	3.7		3.0	8.9	3.9	4.7			0.5	0.5	100.0
8461	D15	5.0	2.0		3.3	3.4		4.6			0.7			3.4	74.9	0.4	1.9	0.3			0.2	100.1
8480	D21	15.2	3.7	15.6		5.1		11.6	3.3		9.4			3.7	28.0	1.4	2.6				0.6	100.2
8996	D31	31.3	2.4		11.1	3.5	0.5	19.3	1.8		0.5	4.0		1.9		22.5				0.4	0.8	100.0
9205	D10	24.0	5.5		4.2	1.0	0.3	8.1				2.1		3.0	21.5	18.4	11.7				0.4	100.2
9228	D22	11.6	2.8		6.8	5.3		12.0			1.5	1.1	2.3	3.6	47.0	1.6	2.7			1.6	0.4	100.3
9235	D1	1.3			1.9	0.2		1.9						1.0	87.4	0.6	1.7	0.1	3.8			99.9
9266	D32	46.5	4.1			2.1		17.1			2.8	5.3		5.1	10.5	2.3	3.7				0.5	100.0
9267	D24	30.5	4.3	6.0		3.4		18.3	4.3		5.2	5.2		4.2	14.5	1.4	1.7			0.4	0.6	100.0
9268	D19	6.1	0.8		2.0	2.1		11.3			2.4	1.9		3.8	63.0	1.8	2.7	1.9			0.2	100.0
9362	D6	26.6	1.5			3.7		10.0	1.8		1.9	4.4		2.4	40.7	0.1	0.7	1.7	3.8	0.4	0.2	99.9
9372	D34	36.2	6.5		5.7	2.1	1.1	26.7	5.2	0.1	2.1	3.9		2.8		3.7	2.7				1.1	99.9
9375	D4	14.5	2.1		8.8	1.9		16.6			4.0	2.7		2.9	41.6	1.7	2.1	0.8			0.3	100.0
9380	D5	15.9	2.0		5.1	4.5		17.4	2.2		5.4	1.9		2.6	38.6	1.1	1.0	1.8			0.4	99.9
9386	D11	23.2	2.5	10.3		6.3		20.6	2.6		3.7	2.1		3.2	21.6	1.0	1.6	0.7			0.7	100.1

Legend

Column Label	Label Description	Column Label	Label Description
Sample No.	AGS sample number	Hem.	Hematite
Site No.	AGS site location number	Kaol.	Kaolinite
Ank.	Ankerite	Micro.	Microcline
Bio.	Biotite	Mont.	Montmorillonite
Brkt.	Brookite	Musc.	Muscovite
ClCh.	Clinochlore	Ortho.	Orthoclase
Dolo.	Dolomite	Paly.	Palygorskite
FlAp.	Fluorapatite	Rhod.	Rhodochrosite
Gyp.	Gypsum		

All values are in weight per cent (wt.%).

SGS Minerals Ltd. performed the analysis.

Software: Bruker AXS Diffrac Plus EVA

The semiquantitative analysis of EVA is performed on the basis of relative peak heights and I/Icor values of those detected crystalline phases with PDF files. Amorphous or crystalline mineral species present in trace amounts may go undetected.

Appendix 3b – X-Ray Fluorescence

Sample No.	Site No.	SiO_2	Al_2O_3	Fe_2O_3	MgO	CaO	Na_2O	K_2O	TiO_2	P_2O_5	MnO	Cr_2O_3	V_2O_5	LOI	Total
		wt. %	wt. %	wt. %	wt. %	wt. %	wt. %	wt. %	wt. %	wt. %	wt. %	wt. %	wt. %	wt. %	wt. %
8135	D8	23.40	6.82	2.81	1.74	30.40	0.29	2.39	0.32	0.26	0.04	0.02	0.01	28.00	96.50
8456	D12	58.20	9.79	4.26	2.39	6.46	0.39	2.60	0.47	0.13	0.02	0.01	0.04	12.70	97.46
8461	D15	11.50	3.27	2.84	1.31	40.60	0.17	1.08	0.11	0.08	0.03	<0.01	<0.01	33.30	94.29
8480	D21	40.60	13.20	4.49	2.64	15.50	0.29	4.00	0.54	0.09	0.06	0.02	0.02	16.40	97.85
8996	D18	49.30	11.50	4.36	5.53	6.78	0.24	4.77	0.63	0.14	0.04	0.02	0.01	13.20	96.52
9205	D10	34.30	6.46	3.95	5.26	19.80	0.59	1.77	0.39	0.09	0.06	0.01	0.02	22.80	95.50
9228	D22	25.40	7.41	4.03	1.77	27.90	0.28	2.34	0.29	0.48	0.08	<0.01	<0.01	24.50	94.48
9235	D1	3.67	0.96	0.58	0.71	49.20	<0.01	0.48	0.05	0.07	0.02	0.01	<0.01	40.60	96.35
9266	D32	59.20	9.50	3.84	2.19	6.92	0.44	2.17	0.45	0.09	0.05	0.02	0.03	11.30	96.20
9267	D24	51.00	11.10	4.27	2.06	8.30	0.38	3.08	0.41	0.12	0.03	<0.01	0.02	15.50	96.27
9268	D19	16.70	6.02	2.16	2.07	36.00	0.16	1.52	0.23	0.08	0.06	<0.01	<0.01	31.20	96.20
9362	D6	37.20	5.85	4.15	1.65	22.60	0.17	1.65	0.24	0.16	0.04	0.01	0.03	22.20	95.95
9372	D34	60.80	16.60	4.89	2.05	0.74	0.52	3.47	0.68	0.09	0.03	0.03	0.04	8.30	98.24
9375	D4	32.80	9.34	2.66	1.55	24.60	0.23	3.58	0.30	0.11	0.05	0.01	0.02	21.50	96.75
9380	D5	34.70	11.50	3.31	2.04	21.10	0.25	3.71	0.44	0.10	0.04	<0.01	0.01	20.10	97.30
9386	D11	43.90	13.30	4.27	2.40	13.50	0.28	2.28	0.60	0.09	0.05	0.02	0.02	14.90	95.61
9266DUP	D32	60.00	9.45	3.81	2.22	6.99	0.46	2.16	0.46	0.10	0.04	<0.01	0.03	11.30	97.02

Legend

Column Label	Label Description	Column Label	Label Description
Sample No.	AGS sample number	TiO_2	Titanium oxide
Site No.	AGS site location number	P_2O_5	Phosphorus oxide
SiO_2	Silicon oxide	MnO	Manganese oxide
Al_2O_3	Aluminum oxide	Cr_2O_3	Chromium oxide
Fe_2O_3	Iron oxide	V_2O_5	Vanadium oxide
MgO	Magnesium oxide	LOI	Loss-on-ignition (amount of material lost due to heating)
CaO	Calcium oxide	Total	Total weight per cent
Na_2O	Sodium oxide	wt. %	Weight per cent
K_2O	Potassium oxide	DUP	Duplicate

Appendix 4 – Duvernay and Muskwa Formations Clay Mineralogy (Qualitative XRD)

Sample No.	Site No.	Sample Type	Crystalline Mineral Assemblage (Relative Proportions Based on Peak Height)			
			Major (>30 wt.%)	Moderate (10-30 wt.%)	Minor (< 10 wt. %)	Trace (< 1 wt. %)
8996	D31	Core	(quartz)		illite, (dolomite)	*chlorite, (*plagioclase), (*potassium-feldspar), (*pyrite), (*brookite)
9205	D10	Core	(calcite)	(ankerite), (quartz)	illite	*(brookite), *(pyrite)
9228	D22	Core	(calcite)		(quartz)	*illite, *chlorite, (*ankerite), (*brookite), (*pyrite), (*potassium-feldspar)
9235	D1	Core	(calcite)			(*quartz), (*gypsum), (*potassium-feldspar)
9266	D32	Core	(quartz)		illite, kaolinite, chlorite, (calcite)	(*ankerite), (*pyrite)
9267	D24	Core	(quartz)		illite, (calcite)	*chlorite, (*mica), (*plagioclase)
9268	D19	Core	(calcite)		illite, (quartz)	*chlorite, (*ankerite), (*potassium-feldspar)
9362	D6	Core	(quartz)	(calcite)	illite	*chlorite, (*mica), (*pyrite), (*apatite), (*gypsum)
9372	D34	Core	(quartz)	illite/montmorillonite mixed	chlorite	*kaolinite
9375	D4	Core	(quartz)	(calcite)	illite	*chlorite, (*ankerite), (*pyrite)
9380	D5	Core		(quartz), illite, (calcite)	chlorite	(*brookite), (*potassium-feldspar), (*rhodochrosite), (*pyrite)
9386	D11	Core	(quartz)		illite, (calcite)	*chlorite, (*plagioclase)

Legend

Column Label	Label Description
Sample No.	AGS sample number
Site No.	AGS site location number
Sample Type	Core, outcrop or cuttings
wt. %	Weight per cent (relative proportion of clay-sized minerals only)

* Tentative identification due to low concentrations, diffraction line overlap or poor crystallinity.

( ) Not a clay mineral according SGS Minerals Ltd.

Appendix 5 – Duvernay and Muskwa Formations Scanning Electron Microscope (SEM) Images and Descriptions

The SEM images in this appendix are thumbnails. Full-size JPGs are in the ZIP file that accompanied this report, available at http://www.ags.gov.ab.ca/publications/abstracts/OFR_2010_02.html.

Duvernay and Muskwa Formations Scanning Electron Microscope (SEM) Images and Descriptions

The SEM descriptions include an interpretation of energy dispersive x-ray (EDX) analysis. Not all of the graphs of the EDX analyses were saved for later interpretation. Therefore, we made the comment 'not saved' within the body of this document, where appropriate.

Majeau Lake Formation, Sample 8479, UWI 100/10-13-063-12W5/00, 8590.5 ft. (2618.4 m) Core Depth

The sample is calcareous, massive dark grey shale with poker-chip fractures. The sample was taken in a rubble zone.

Image	Magnification
8479_1	25×
8479_2	100×
8479_3	250×
8479_4	1000×
8479_5	800×
8479_6	10 000×
8479_7	2500×
8479_8 (backscatter)	500×
8479_9	500×

Image **8479_1** (25× magnification) is a low-magnification view of homogeneous, clay-rich shale with a few scattered coarse grains. The fracture in the northeast corner of the sample is likely induced.

An EDX overview of image **8479_2** (100× magnification) indicates the presence of potassium-rich clay and a significant amount of calcite. A strong north-northeast bedding trend is evident, and the sample appears to be well compacted. Porosity is dominated by apparent lenticular micropores ~100 µm or wider and ~5 µm in height.

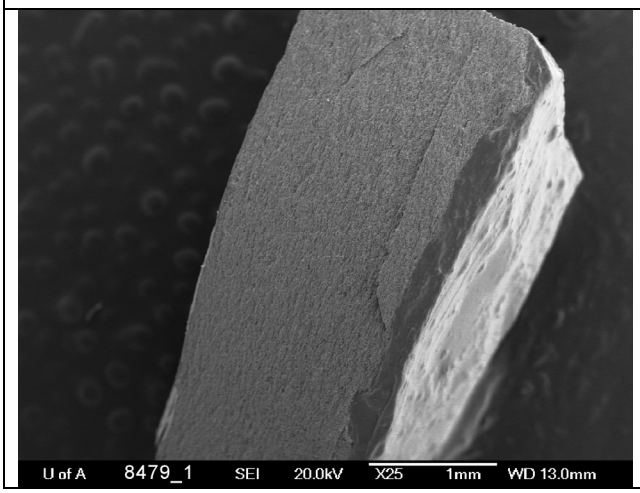

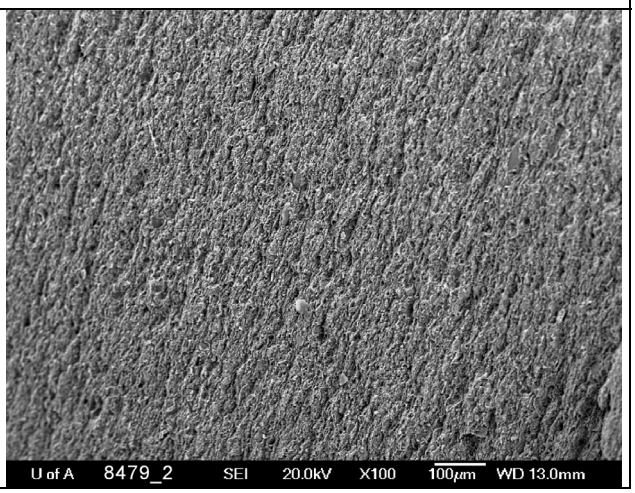

Image **8479_3** is a 250× magnification image of the previous image and appears to be very homogeneous with few distinguishing features. There appears to be a considerable amount of porosity that is generally less than ~10 µm in diameter; some of the pores now appear to be circular.

At 1000× magnification (image **8479_4**), a significant amount of grain plucking is evident in the form of open circular pores. We therefore believe that some of the larger, apparent slit-like pores are due to grain plucking. Most of the circular pores are less than 10 µm in diameter.

An EDX analysis was done on a number of grains in images 8479_4 and 8479_5 (see 'Composition Table Sample 8479' at the bottom of this sample description**)**. Results indicate the presence of calcite, clay of the illite-smectite family, biotite/muscovite, quartz and dolomite.

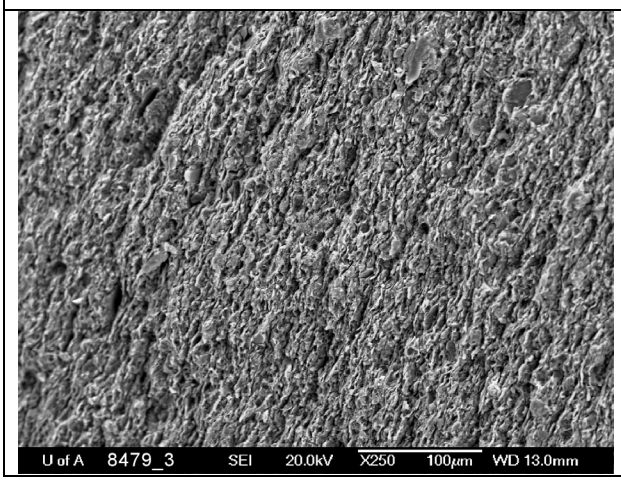

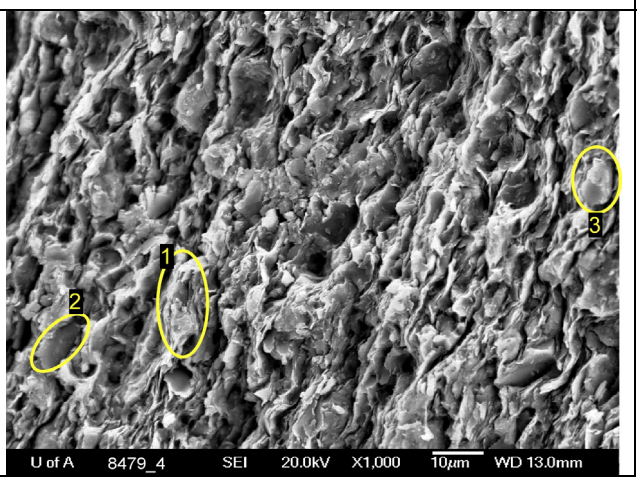

Image **8479_6** is a 10 000× magnification image of image **8579_5** (800× magnification) that focuses on the development of apparent porosity between grain surfaces. The material is dominated by clay minerals, likely of the illite-smectite family. The open linear pores, elongated north-south in the image, occur at grain boundaries and may be due to relaxation of the sediment upon unloading, which would fit the 'poker-chip' appearance of the core. Circular pores may be sites of plucked gains, so it is difficult to be certain of porosity development in this image.

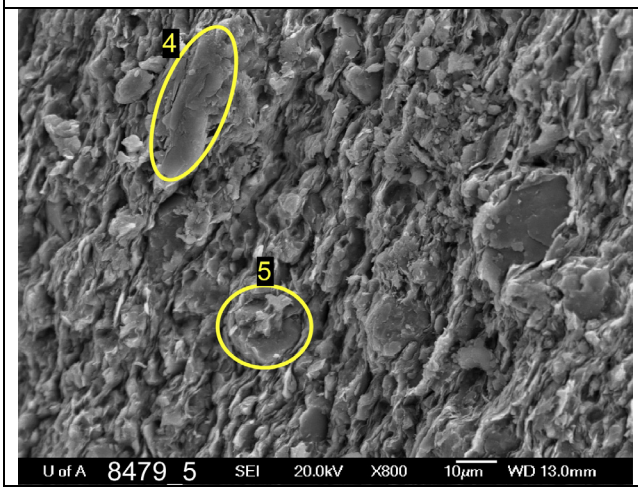

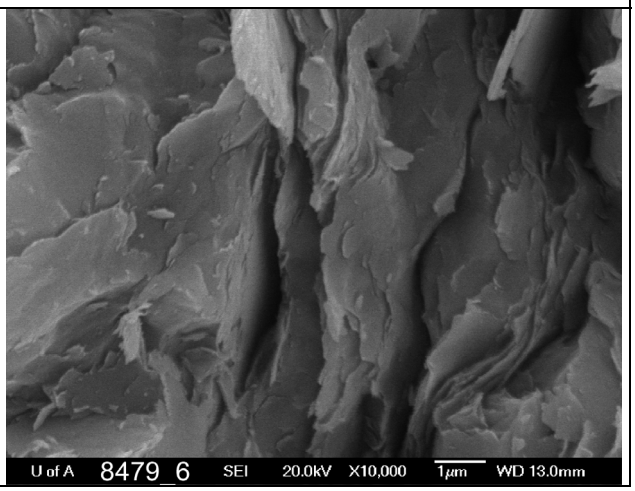

Image 8479_7 is a 2500× magnification view of a pyrite framboid wrapped in clay. Open circular pores, 1–3 µm in diameter, are evident throughout the sample and likely represent plucked grains. Linear, open pores striking north are likely due to expansion during core unloading.

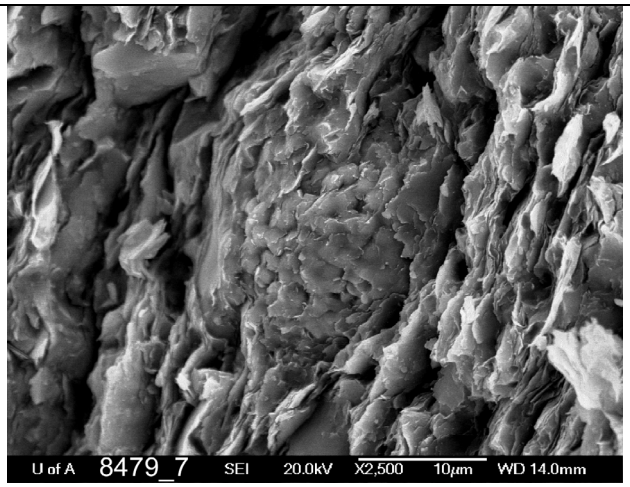

Image **8479_8** (500× magnification) is a backscatter image of **8479_9** (500× magnification). Pyrite framboids are evident in the centre and centre-right of the image (yellow circles), and single pyrite crystals are also present (red circles). Generally speaking, pyrite is not abundant in this sample. There may be more heavy minerals identified by backscattering in this image than we have pointed out. Ideally, the sample would be coated with chromium for maximum effectiveness for backscattering, but these samples are coated with gold because our purpose was primarily shale mineralogy and sedimentology.

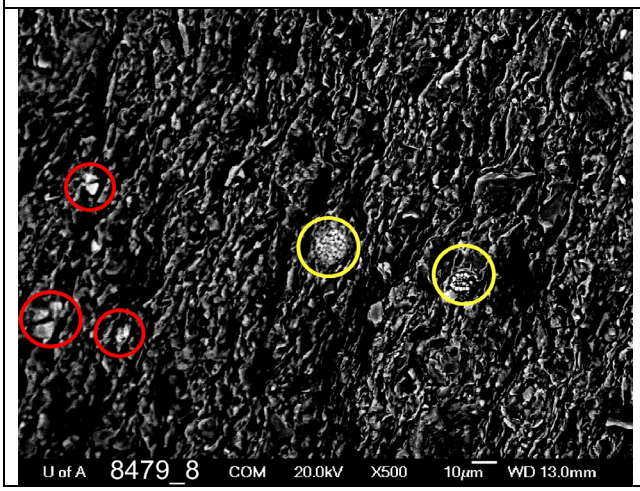

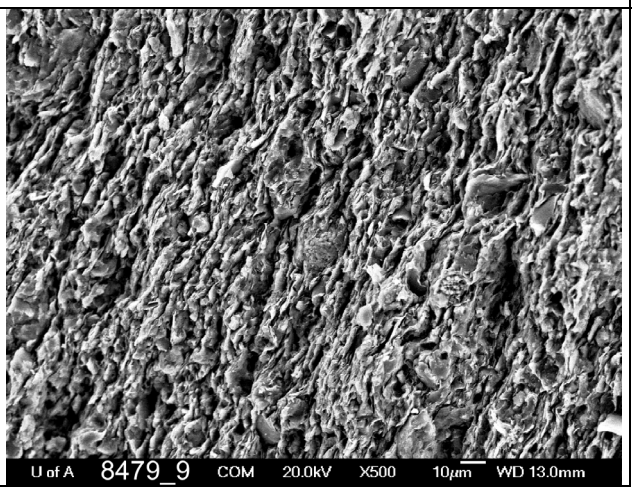

EDX results for sample 8479

Composition Table Sample 8479	Image	ID on Image
Calcite dominant with illite/smectite (8479_EDX_002)	8479_4	1
Biotite/muscovite (8479_EDX_003)	8479_4	2
Quartz (8479_EDX_004)	8479_4	3
Biotite/muscovite (8479_EDX_005)	8479_5	4
Dolomite (8479_EDX_006)	8479_5	5
Pyrite (8479_EDX_007)	8479_6	6

Note: The depth of penetration of the EDX analysis is about 1–2 μm, so the chemistry below the surface may dominate the surface mineral.

Duvernay Formation, Sample 9208, UWI 100/09-06-052-11W5/00, 9904 ft. (3018.7 m) Core Depth

The sample is firm, massive, calcareous black shale.

Image	Magnification
9208_1	25×
9208_2	100×
9208_3	250×
9208_4	1000×
9208_5 (Backscatter)	1000×
9208_6	6500×
9208_7	10 000 ×
9208_8	3700×
9208_9	1600×

Image **9208_1** (25× magnification) is a low-magnification view of homogeneous, calcareous black shale. Bedding trend is northeast in all images. Images 9208_2 and 9208_3 are higher magnification views.

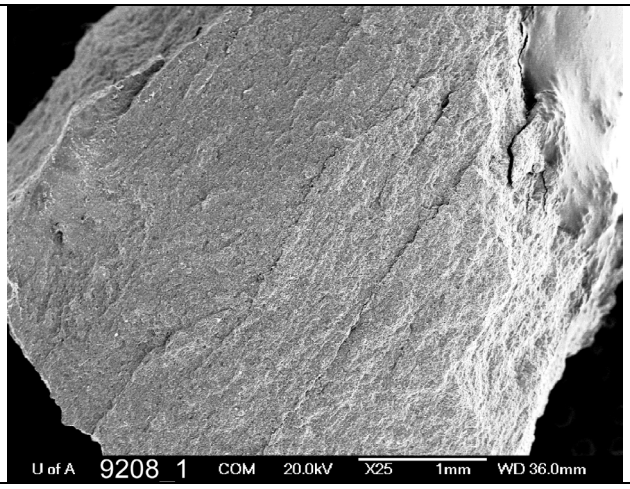

An EDX analysis overview of image **9208_2** (100× magnification) shows a dominance of calcite with a mixture of clay (illite?) and perhaps quartz. The EDX calcium peak is so strong that perhaps the sample should be called an argillaceous carbonate mudstone. A few floating, dark-coloured grains can be seen in image 9208_2. Whereas image **9208_3**, at a higher magnification (250×), has a somewhat grainy texture.

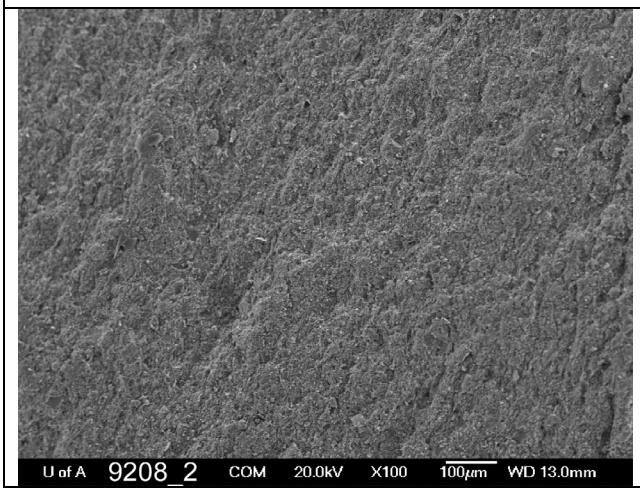

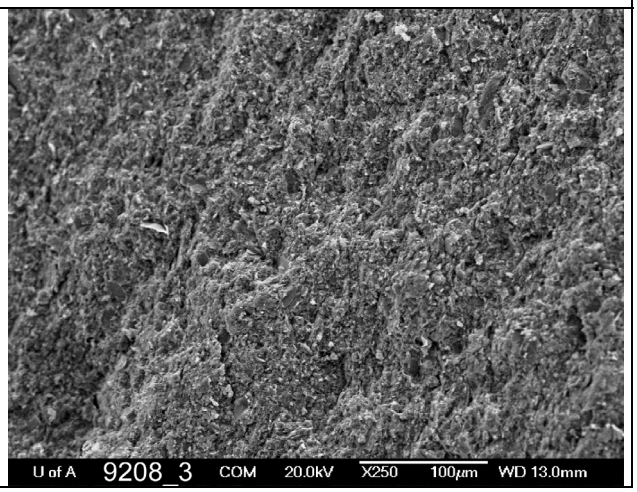

At 1000× magnification in image **9208_4**, there appears to be a high proportion of silt-sized particles, perhaps as much or more silt than clay. Image 9208_8 is a higher magnification view of this site.

In image 9208_4, the silt does not appear to be concentrated in laminae. The alignment of the clay sheets suggests a weak north-northeast bedding trend. An EDX analysis indicates the presence of calcite grains (primary?) identified at site 1. A few other particles of similar morphology can been seen elsewhere in the image. A clay and calcite mixture at sites 2 and 3 is evident from the EDX analysis. Yellow and red arrows indicate the locations of images 9208_6 and 9208_7, respectively.

Image **9208_5** (1000× magnification) is a backscatter image of 9208_4 that shows a lack of heavy minerals in the sample. Some of the larger circular or semicircular particles may be pyrite (e.g., extreme upper right), but there is a general lack of pyrite in this sample. There may be more heavy minerals identified by backscattering in this image than we have indicated.

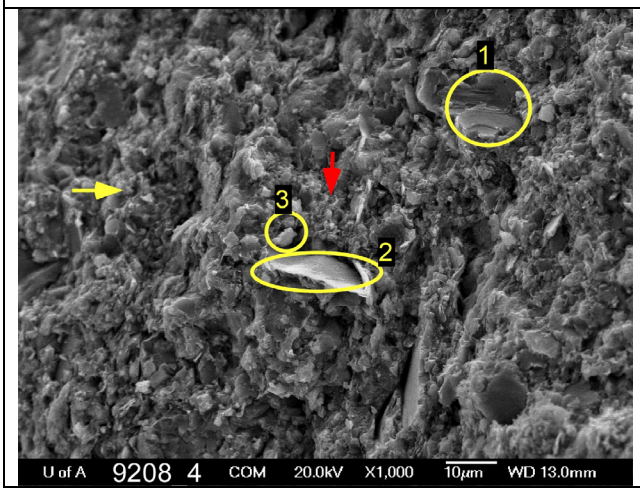

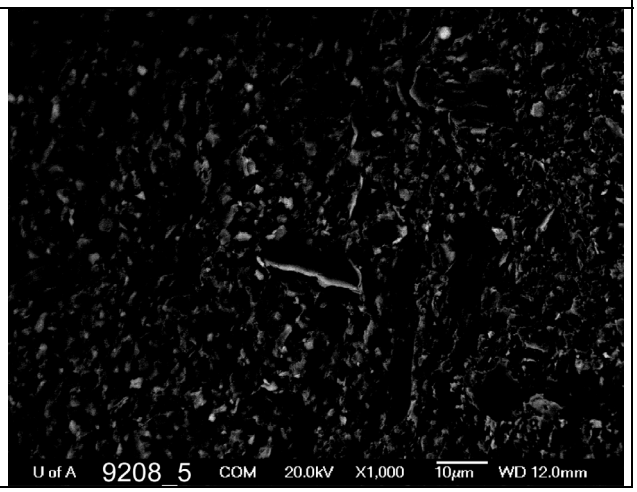

EDX analysis identified calcite particles ('Ca') in image **9208_6** (6500× magnification). The black arrows point to clay sheets, a minor presence in this view.

Image **9208_7** (10 000× magnification) also appears to be dominated by calcite; however, many of the grains are coated with clay.

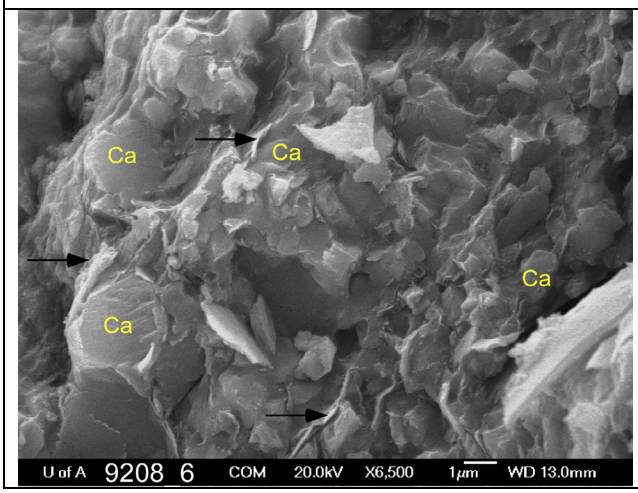

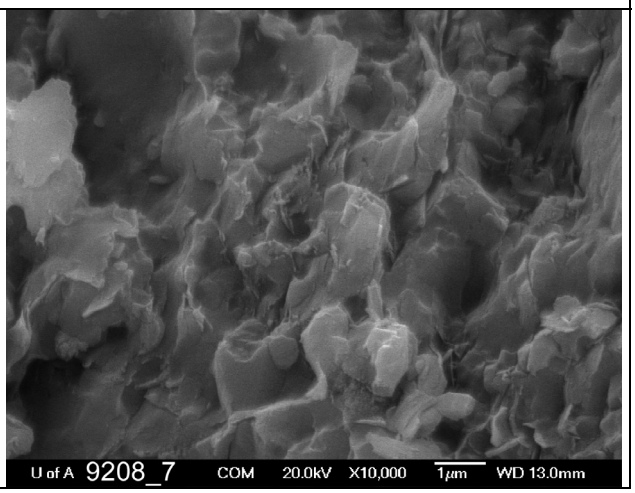

The focal points of image **9208_8** (3700× magnification) are the large, perhaps authigenic, calcite particles (see image 9208_4 and 9208_EDX_002) surrounded by clay and the quartz particle in the yellow circle. Quartz grains are difficult to locate in this sample. There is a high degree of porosity relative to image 9208_7. Pore sizes range from <1 µm to 4–5 µm; porosity is very well distributed.

Image **9208_9** is a relatively low magnification (1600×) image of an area of fairly high, well-distributed porosity. Mineralogy is again dominantly calcite and clay of various sizes.

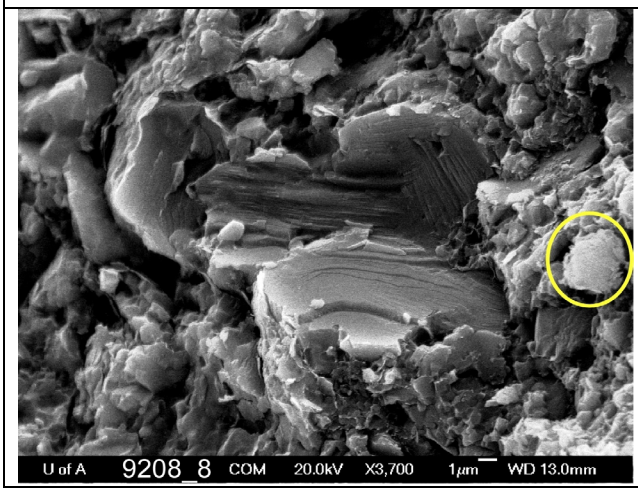

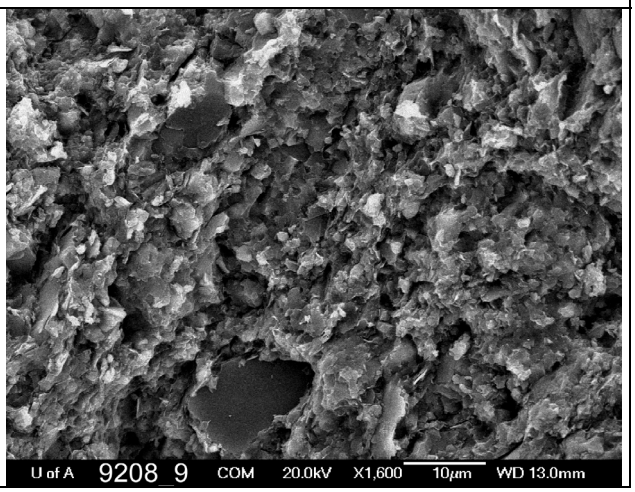

EDX results for sample 9208

Composition Table Sample 9208	Image	ID on Image
Calcite (9208_EDX_002)	9208_4	1
Clay, probably illite, with calcite (9208_EDX_8692S_003)	9208_4	2
Calcite and some clay (illite; 9208_EDX_004)	9208_4	3
Calcite (9208_EDX_005)	9208_6	Ca
Quartz (9208_EDX_006)	9208_8	Circle

Note: The depth of penetration of the EDX analysis is ~1–2 µm, so the chemistry below the surface may dominate the surface mineral if the surface material is very fine grained or thin.

Ireton Formation, Sample 9232, UWI 100/10-21-061-01W5/00, 4833 ft. (1473.1 m) Core Depth

The sample is black, firm, massive carbonate mudstone with brachiopod fragments.

Image	Magnification
9232_1	23×
9232_2	100×
9232_3	500×
9232_4	2500×
9232_5	7500×
9232_6	4000×
9232_7	1000×
9232_8	2000×
9232_9	1500×

Image **9232_1** is a low-magnification (23×) overview of the Ireton sample. Bedding trends north. The sample appears massive. The EDX overview suggests the sample is dominated by calcite and, to a lesser extent, clay of the illite-smectite family, with perhaps some dolomite. Porosity is evident at this scale of magnification in the form of dark spots on the image.

Image **9232_2** (100× magnification) also appears massive, with porosity showing up as dark spots throughout the image. The largest pores are ~40 µm in diameter on the left side of the image. There are at least two fractures visible at this scale that trend in the same direction as the bedding, as indicated by the white arrows.

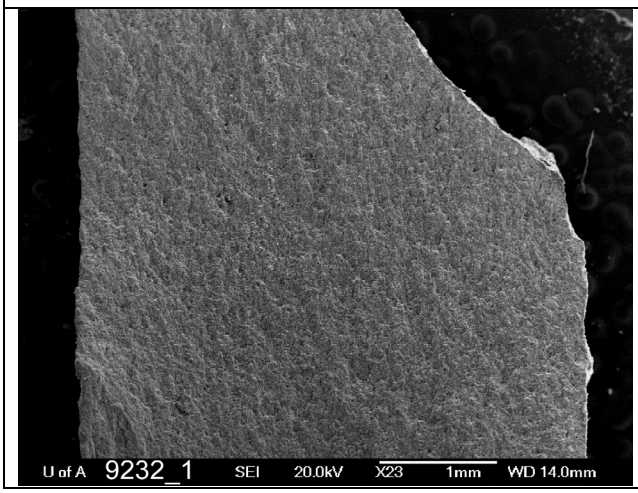

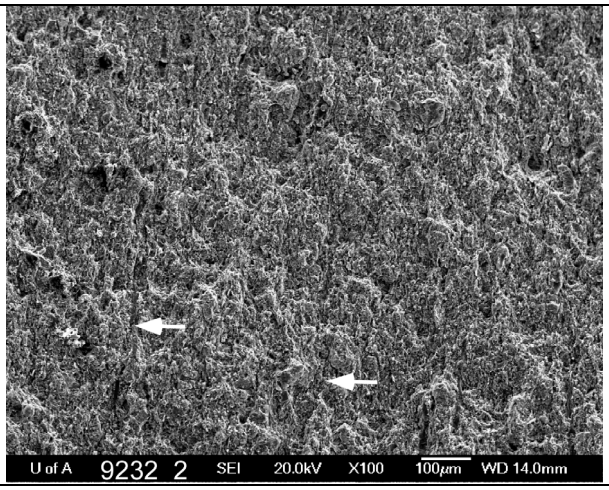

An EDX analysis of image **9232_3** (500× magnification) yielded the same result as the first EDX analysis. Calcite appears to dominate the mineralogy, with subordinate clay and dolomite. The fabric shows a fairly strong vertical linear trend with a substantial amount of porosity. Some of the pores have a linear trend parallel to the bedding. The yellow box identifies the location of image 9232_4. The numbers '6' and '7' identify the locations of images 9232_6 and 9232_7, respectively.

An EDX analysis of image **9232_4** (2500× magnification; the image is slightly out of focus) reveals an interesting mineralogy. At point '1,' the analysis shows a mixed mineralogy somewhat similar to the previous analyses. The EDX resolution is ~1 µm in diameter and depth, so the particle may be thin, resulting in minerals behind the relatively flat particle showing up on the EDX graph.

The graph displays a mineralogy high in silicon and aluminum, with a little potassium (illitic clay), but also high iron and sulphur (probably pyrite), high magnesium (dolomite?) and low calcium. At this magnification, it is likely that the grains behind the flat particle are rather small.

At point '2' on the image, the analysis displays a mineralogy high in silicon and aluminum with a little potassium (illitic clay?), high calcium (calcite) and much lower iron and sulphur (pyrite), and magnesium.

Point '3' shows a very strong calcite and clay response. Pore morphology in image 9232_3 is displayed as lineations up to ~7–10 µm in length, with smaller pores a few micrometres in diameter. There is a strong sense of particles being wrapped in clay, as seen at the white arrows.

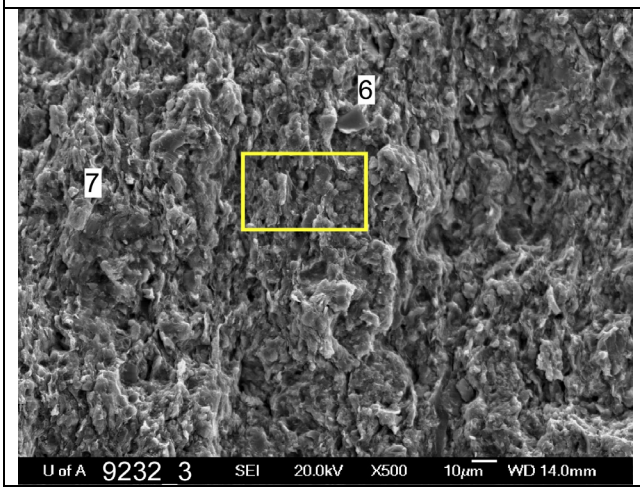

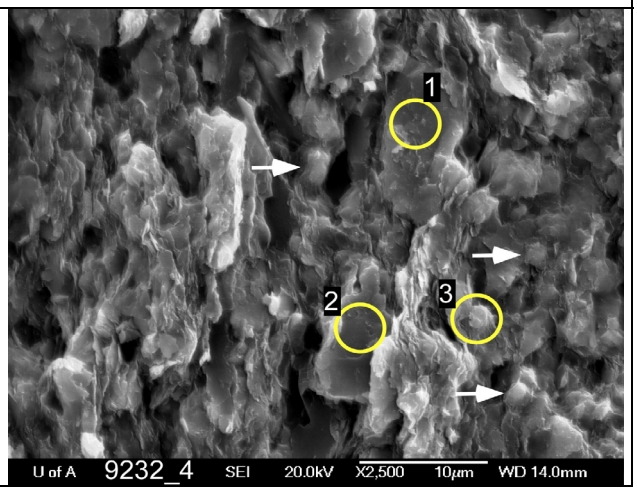

Image **9232_5** (7500× magnification) gives a very good sense of the sample's fabric. The nodular appearance is clear. Particles are wrapped in clay and range in diameter from 1 µm to more than 4–5 µm. The red arrow points to a particle that may be a nodule wrapped in clay, although we are not entirely certain if the material wrapping the particle is clay. Linear pores are seen on the right side of the image (white arrow), but this may be a fresh fracture (i.e., induced during core retrieval) because the sides of the pore appear to fit together in some areas.

The location of image **9232_6** (4000× magnification) can be seen on image 9232_3 just above the yellow box on the right side. Mica and calcite grains are present, along with a substantial amount of clay. The porosity in this image is dominated by pores much less than 1 µm in diameter. The white arrow identifies a fracture.

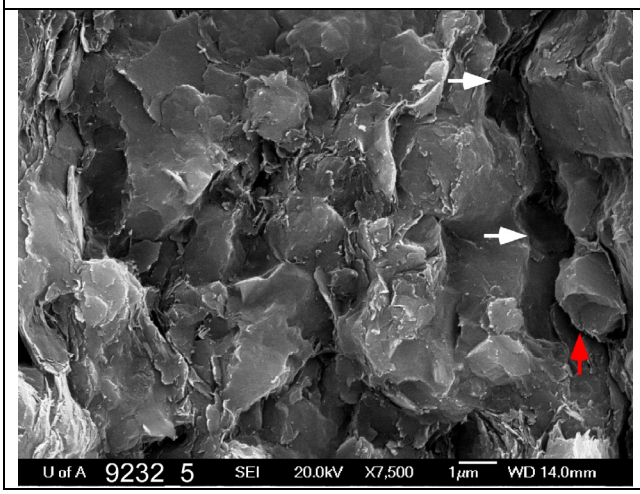

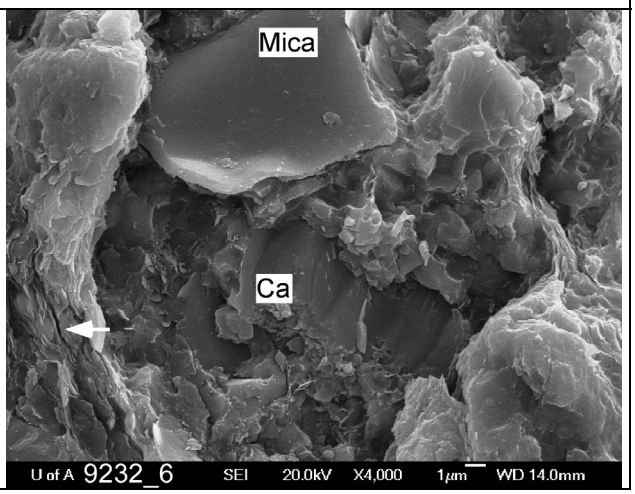

Image **9232_7** (1000× magnification) again shows the well-cemented fabric of the sample and reveals a surprising amount of porosity. The lithological classification of the sample, based on the previous images, would be an argillaceous carbonate mudstone but with the carbonate particles being dominantly nodules. A rough estimation of the amount of carbonate versus clay in the sample would be ~70%–80% carbonate and ~20%–30% clay. The arrow identifies the location of image 9232_8.

In image **9232_8** (2000× magnification), the EDX analysis (not saved) suggests the material is dominated by carbonate and clay. There is a variety of sizes and shapes of pores in this view. The open space at the yellow arrow, however, may be a fracture at a grain contact.

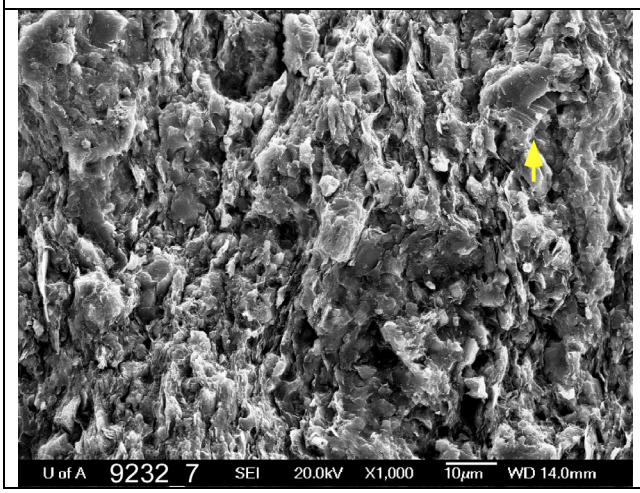

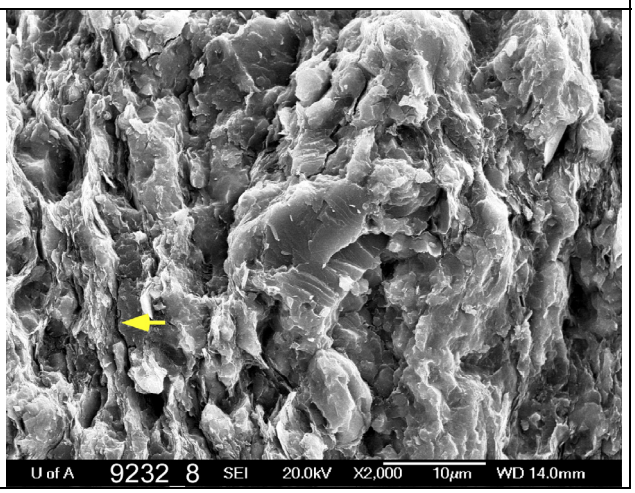

The particle in the centre of image **9232_9** (1500× magnification) is quartz. The surrounding material is well cemented with little porosity and consists, in large part, of many small particles.

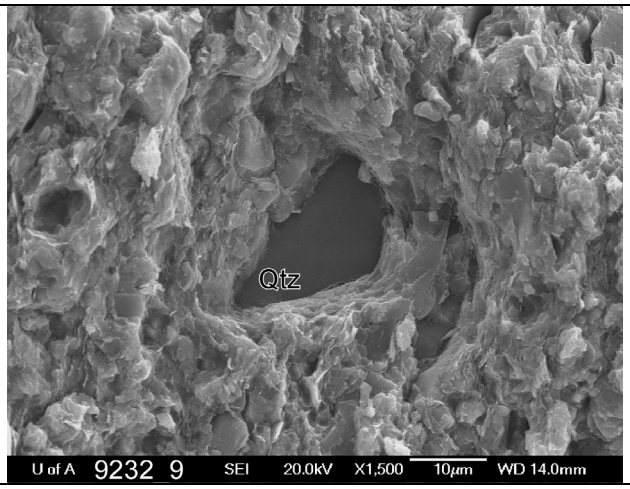

EDX results for sample 9232

Composition	Image	ID on Image
Calcite, clay (illite/smectite), dolomite (9232_EDX_002)	9232_3	None
Mixed mineralogy of clay, pyrite and lesser dolomite and calcite (9232_EDX_003)	9232_4	1
Mixed mineralogy of clay, calcite and lesser pyrite and dolomite (9232_EDX_004)	9232_4	2
Calcite and clay (9232_EDX_005)	9232_4	3
Mica (9232_EDX_006)	9232_6	Mica
Calcite (9232_EDX_007)	9232_6	Ca
Quartz (9232_EDX_008)	9232_9	Qtz

Note: The depth of penetration of the EDX analysis is about ~1–2 μm, so the chemistry below the surface may dominate the surface mineral.

Duvernay Formation, Sample 9238, UWI 100/06-14-037-07W5/00, 3649.7 m Core Depth

The sample is very firm shale with fine laminations <1 mm thick. This is the second deepest sample of the Duvernay Formation in our study.

Image	Magnification
9238_1	25×
9238_2	95×
9238_3 (backscatter)	250×
9238_4	250×
9238_5	400×
9238_6	1000×
9238_7	6000×
9238_8	10 000×

Image **9238_1** is a low-magnification (25×) view with the bedding trending approximately north. There is a fracture traversing the middle of the sample in the same direction as the bedding. The texture is fairly homogeneous. There is little porosity at this magnification, although there are dark spots scattered throughout the sample.

Image **9238_2** (95× magnification) was taken in the middle of image 9238_1 (inside the large yellow square). The fracture is again evident in the centre of the view. Porosity appears to be distributed throughout the sample, with perhaps a weak alignment along the bedding trend. An EDX overview on image 9238_2 indicated that clay minerals (probably illite) and to a lesser extent calcite are dominant. The smaller square identifies the location of images 9238_3 and 9238_4.

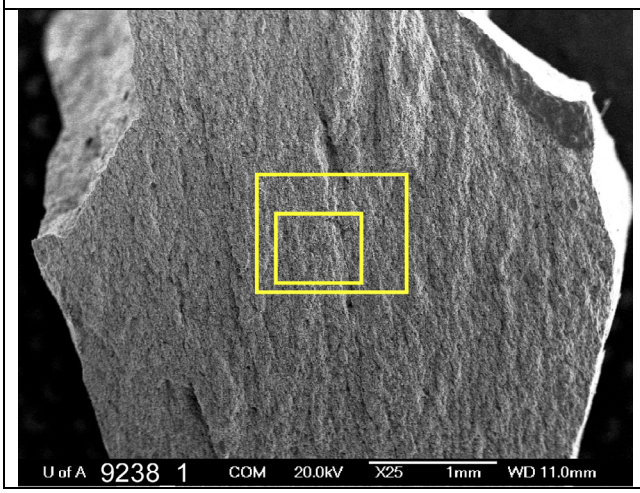

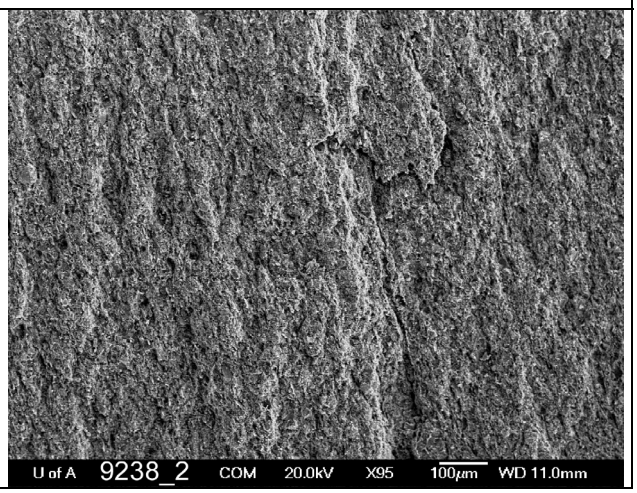

Image **9238_3** (250× magnification) is a backscatter image of 9238_4. Pyrite framboids are evident in the lower portion of the image (yellow squares). There are possibly single-crystal pyrite grains (or other heavy minerals) in the circles. There may be more heavy minerals identified by backscattering in this image than we have indicated.

Image **9238_4** (250× magnification) has a grainy texture with some large (10–20 µm diameter) grains scattered throughout the image, which are investigated in images 9238_5 and 9238_6. The rectangle identifies the location of image 9238_5. The arrows point to the locations of the grains examined in the next few images.

Porosity in image 9238_4 is quite significant and are examined more closely in images 9238_7 and 8.

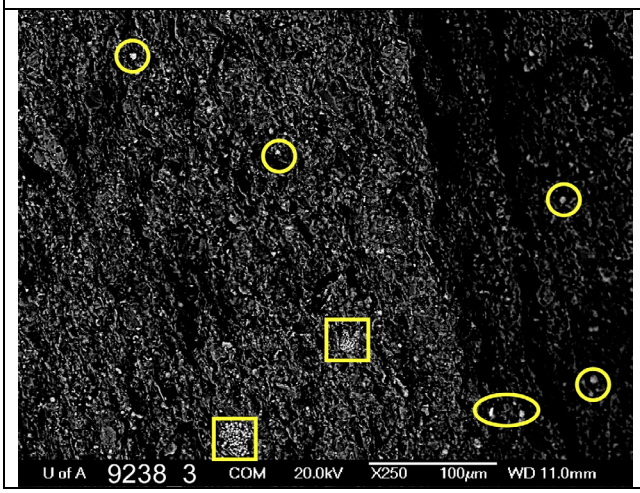

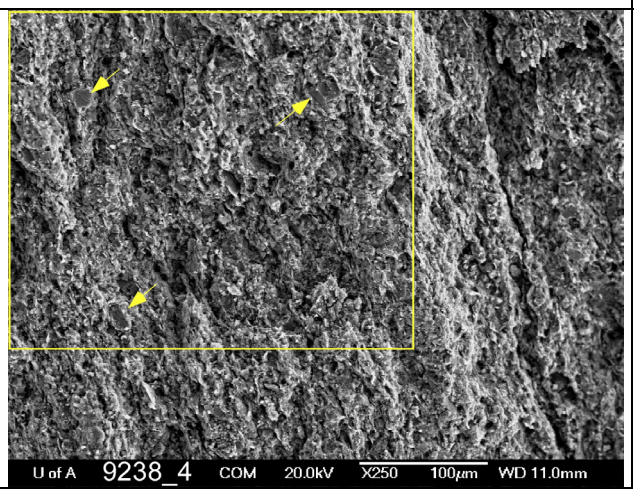

An EDX analysis of the grains in the two circles on image **9238_5** (400× magnification) identified potassium feldspar, and the grain in the square is dolomite. The red arrow identifies a small fracture. The yellow arrow indicates the location of image 9238_6.

An EDX overview of image **9238_6** (1000× magnification) revealed calcite, dolomite and a framboidal pyrite grain. The clay-dominated matrix between the grains was also analyzed, revealing an illite-type clay but with feldspar grains beneath the cover of clay. There is a weak north-south lamination of the clay in this image. No quartz was detected in any of the images of sample 9238. The arrow identifies the location of image 9238_7.

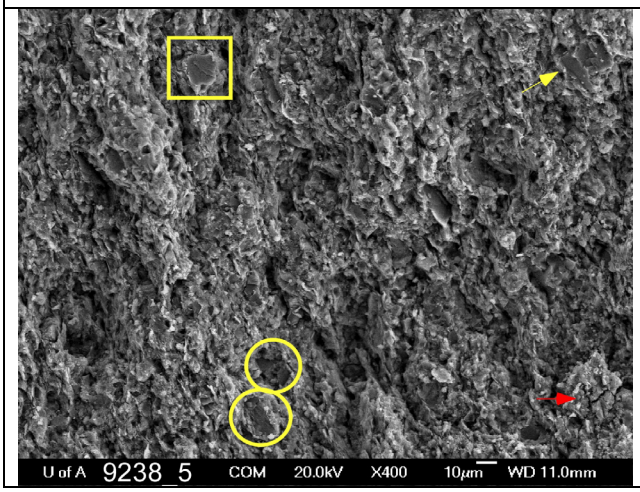

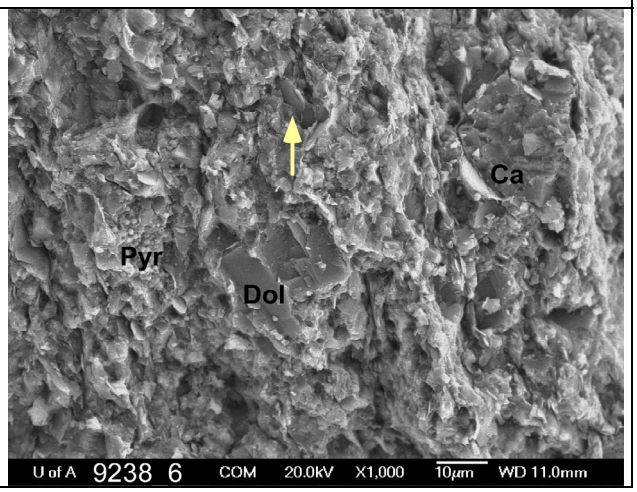

Images **9238_7** (6000× magnification) and **9238_8** (10 000× magnification) are high-magnification views of matrix porosity and mineralogy. An EDX overview identified mica, calcite, feldspar and illite in image 9238_7, with most of the grains being calcite and potassium-rich feldspar.

A loosely packed cluster of calcite grains with a high degree of porosity dominates image 9238_8. The loose particles of calcite and clay likely spalled off during SEM preparation. The calcite grains range from ~1 µm to ~3–4 µm in diameter. The yellow circle highlights a relatively rare view of an oil meniscus.

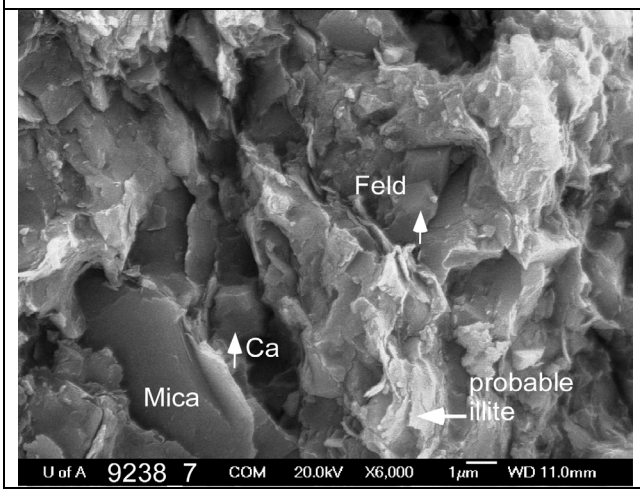

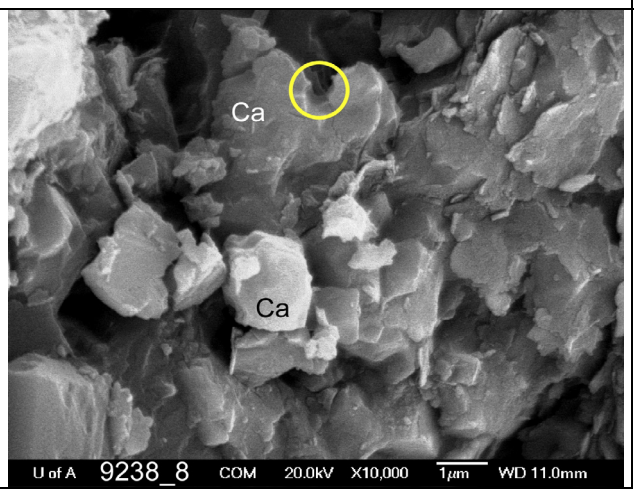

EDX results for sample 9238

Composition	Image	ID on Image
Feldspar (9238_EDX_002)	9238_5	Circle
Dolomite (9238_EDX_003)	9238_5	Square
Pyrite, dolomite, calcite and feldspar (EDX not saved)	9238_6	Pyr, Dol, Ca
Mica, calcite, feldspar and illite (EDX not saved)	9238_7	Mica, Ca, Feld
Calcite	9238_8	Ca

Note: The depth of penetration of the EDX analysis is ~1–2 µm, so the chemistry below the surface may dominate the surface mineral.

Duvernay Formation, Sample 9365, UWI 100/02-06-047-04W5/00, 8687 ft. (2647.8 m) Core Depth

The sample is black calcareous shale with rare 1–2 mm laminations. Calcite-filled vertical and diagonal fractures with slickensides are evident in the core. In the left photo, the sample lies in the core box on the far right.

Image	Magnification
9365_1	25×
9365_2	100×
9365_3	250×
9365_4	6000×
9365_5 (backscatter)	450×
9365_6	2500×

Image **9365_1** is a low-magnification (25×) view of the sample, with bedding trending approximately north. Very little porosity is evident at this magnification.

Image **9365_2** (100× magnification) was taken almost in the centre of the last image. The surface appears to have a grainy texture with little or no indication of bedding. Porosity is very low to absent in this view. The yellow box outlines the area of image 9365_3.

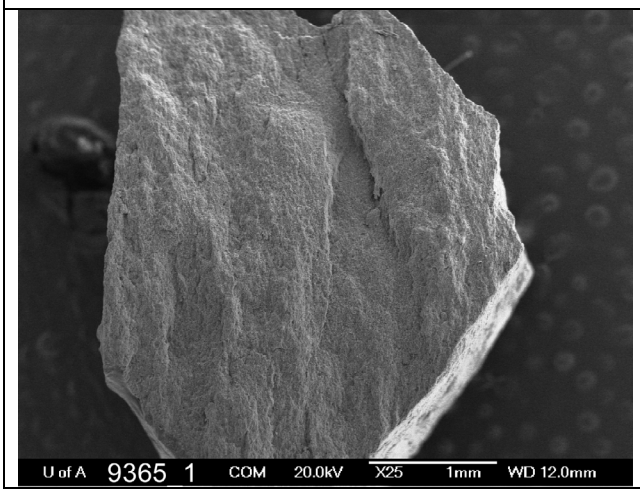

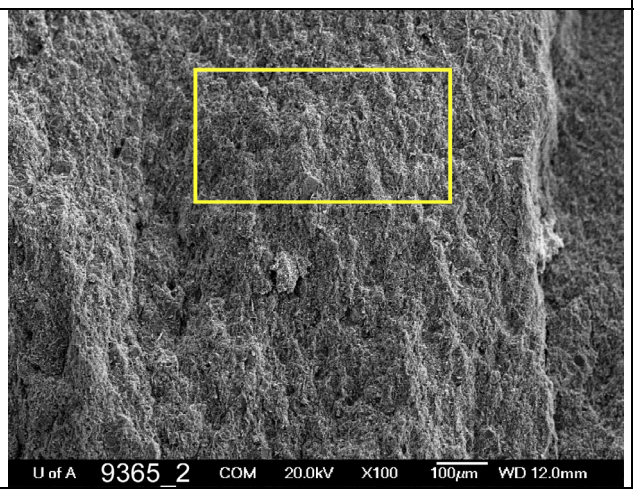

An EDX overview of image **9365_3** (250× magnification) indicated that it is a calcite-rich sample with illite-type clays. Fracturing (indicated by the arrow) is evident, although the fractures appear fresh.

An EDX overview of image **9365_4** (6000× magnification) indicated the presence of quartz and calcite. The quartz particles are aligned and may form part of a single-grain lamina. The upper quartz particle appears to be covered with clay. The pore toward the upper left of the calcite particle may be a plucked grain, but we are not certain of this interpretation. There is some porosity evident, although the pores are <1 µm in diameter. Open spaces near grain boundaries may be due to pressure relaxation after retrieval of the core.

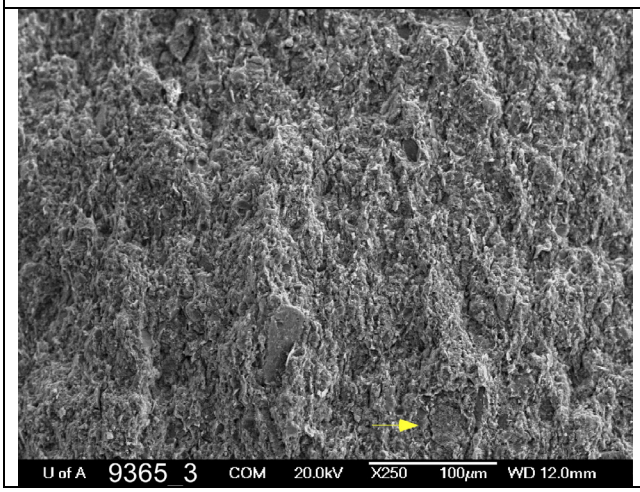

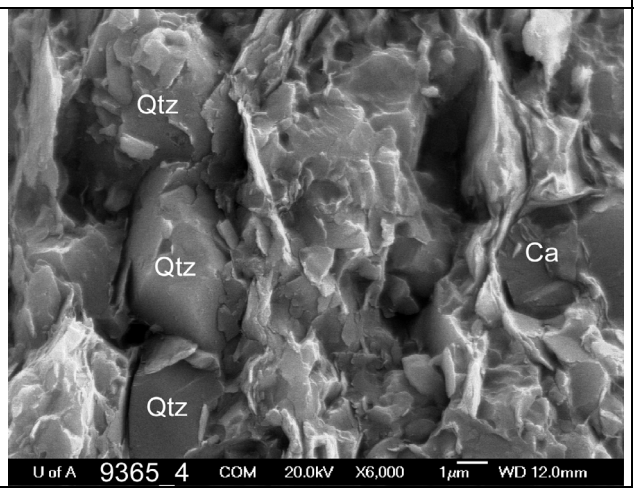

Image **9356_5** is a backscatter image at 450× magnification. The location of the image is in the lower central portion of image 9365_3. A heavy mineral, most likely pyrite, is identified by the circles. Both framboidal pyrite and single pyrite crystals appear to be present.

Image **9356_6** is a high-magnification (2500×) view of the sample's microporosity. The mineralogy is dominantly calcite grains and illite-type clay, with many calcite grains wrapped in clay. In fact, there is very little porosity present; much of what there is being linear along grain boundaries or between clay sheets. Hence, the connectivity of the porosity appears poor, although this is conjecture.

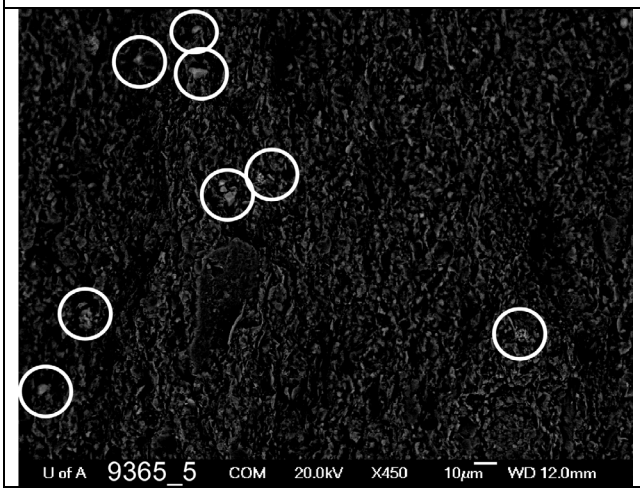

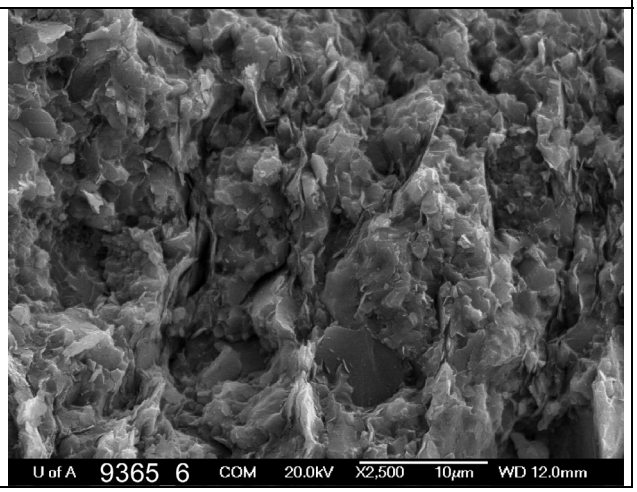

EDX results for sample 9365

Composition	Image	ID on Image
Quartz (9365_EDX_002)	9365_4	Qtz
Calcite (9365_EDX_003)	9365_4	Ca
Pyrite (9365_EDX_005)	9365_5	Circles
Note: there is no EDX_004		

Note: The depth of penetration of the EDX analysis is ~1–2 μm, so the chemistry below the surface may dominate the surface mineral.

Muskwa Formation, Sample 9370, UWI 100/02-04-126-11W6/00, 1523.6 m Core Depth

The sample is very fissile, silty, friable black shale with ‘hockey puck’ fractures.

Image	Magnification
9370_1	25×
9370_2	100×
9370_3	250×
9370_4 (backscatter)	250×
9370_5	850×
9370_6	2700×
9370_7	1000×
9370_8	2000×
9370_9	1700×

Image **9370_1** is a low-magnification (25×) view with bedding trending approximately east. There is a fresh fracture traversing the middle of the sample in the same direction as the bedding. The fracture bifurcates and rejoins along the path, as indicated by the two red arrows. The texture is fairly homogeneous and has a grainy appearance. There is visible porosity at this magnification.

An EDX overview of image **9370_2** (100× magnification) indicates that potassium-clay minerals (illite) dominate. Very little calcite is present. The fractures are again visible. There is a strong east-west component to the bedding. The yellow arrow points to the location of image 9370_3. The area identified by the red arrow is not a feature but a reflection from overcharging, as indicated by the following images.

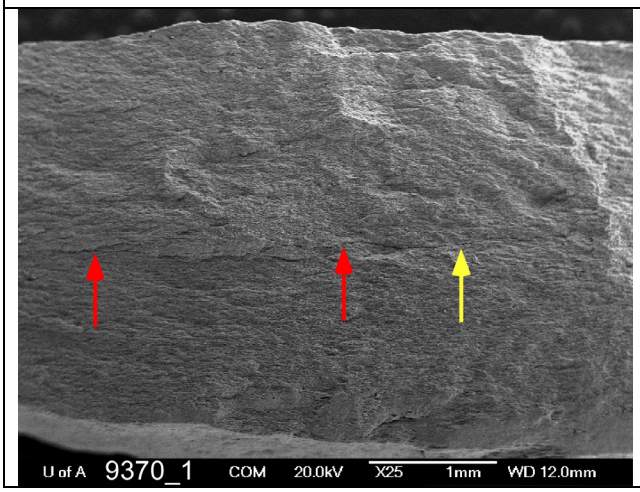

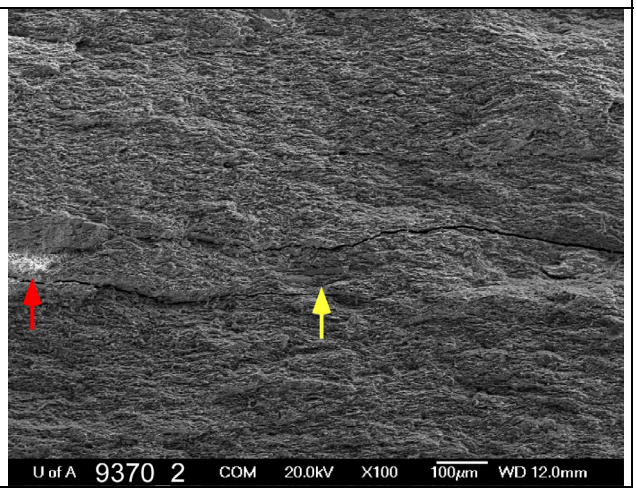

Image **9370_3** is a 250× magnification that examines the linear feature in the lower centre of the image (yellow arrow).

Image **9370_4** (250× magnification) is a backscatter image with two pyritized shell fragments (sponge spicule?) apparent in the lower centre (yellow arrow). An EDX analysis on the particles confirmed they are pyritized. The bright white areas of the image (yellow circles) are pyrite crystals that appear, at this scale of magnification, to be single nodules rather than framboids. The mineralogy of many of the small (~2–5 µm) white grains in this image is unknown. The white area identified on image 9370_2 does not show up as a heavy mineral, specifically pyrite. Open, fresh fractures are visible above and below the pyritized fragment.

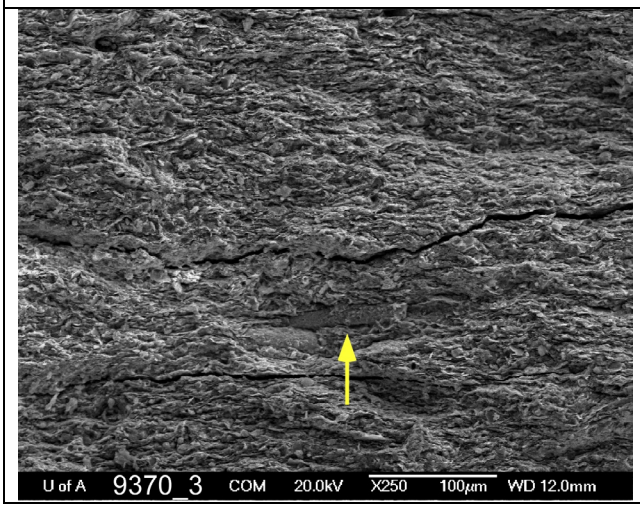

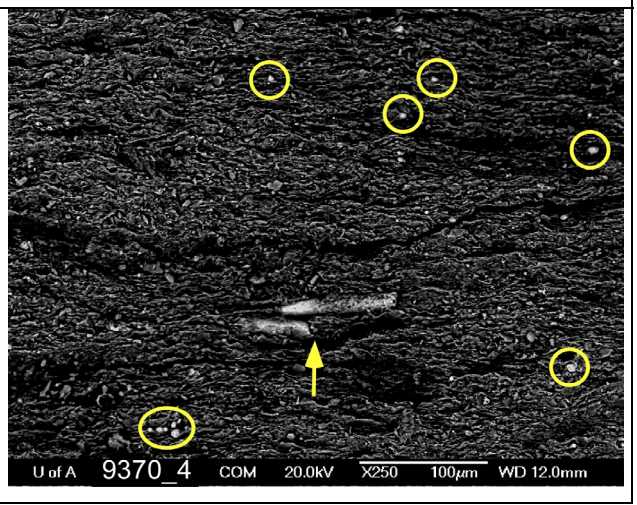

Image **9370_5** (850× magnification) is a close-up image of the shell fragments in image 9370_3. The fragments have a relatively rough-pitted surface and are somewhat coated with clay. The larger fractures (red arrows) above and below the fragments are now clearly visible and appear fresh. The image also reveals more fractures (yellow arrows) along planes of weakness, presumably bedding planes. This is also the first close-up view of the clay. The flakiness apparent in this image provides evidence of the sample's fissility. There are also many silt-sized particles in the clay (white arrows), as the next few images will show. The right upper white arrow indicates the location of image 9370_6.

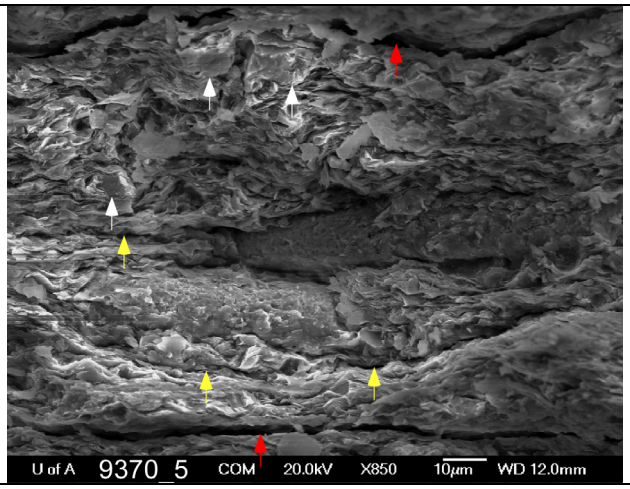

Images **9370_6** (2700× magnification) and **9370_7** (1000× magnification) concentrate on the texture and mineralogy of the sediment.

Image 9370_6 is taken in the upper centre of image 9370_5. The sample is very fissile, as evidenced by the presence of numerous clay flakes. An EDX analysis identified the clay as illite. There are numerous plucked grains (identified by the white arrows). The particles are about 2–3 µm in diameter, and we classified them as large clay-sized particles. The potassium feldspar grain in the upper left is about 12 µm across, with poor sphericity and subrounded to subangular edges. The clay sheets below the particle are clearly compressed.

We need to be careful interpreting the textural and mineralogical influences on porosity because of the extreme fissility of the sample. For example, porosity is apparent between many clay sheets, but relaxation of the sample upon unloading of the core may have had an influence. The large quartz particle (EDX not saved) has occluded porosity below the grain by compressing clay sheets. This can also be seen in image 9370_5 below the particles identified by the upper two white arrows. In the latter case, there does not appear to be porosity on either side of the particles. There does, however, appear to be porosity between the particles due either to the proximity of the particles (little room for clay to settle) or to particle relaxation resulting from core unloading, which would have caused the clay sheets to spall.

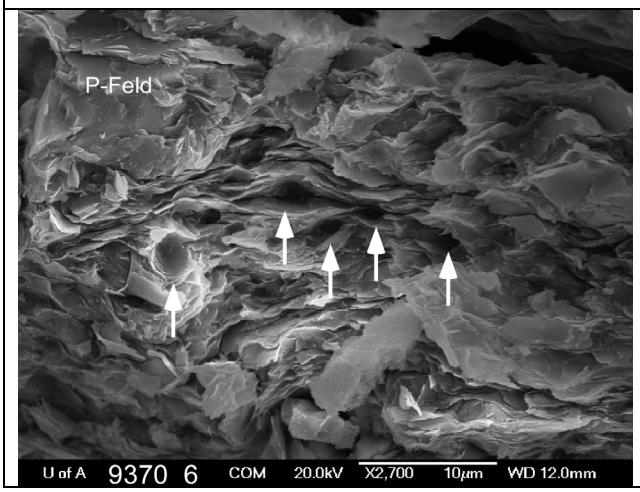

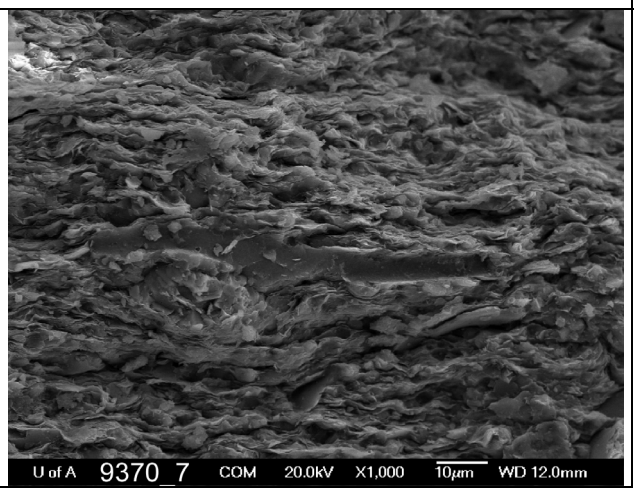

The large linear particle in the centre of image **9370_7** (2000× magnification) is a mould of a plucked particle, consisting of illite that wrapped around the particle. A key question concerning porosity in this sample concerns the influence that small clay-sized particles had on the magnitude and distribution of porosity. Image 9370_7 has a strong east-trending fabric with a very high degree of clay-sized and lower silt-sized particles of non–clay minerals. Porosity between clay sheets appears to be high, but this may be the result of relaxation of the layers due to core unloading. Nonetheless, porosity appears to be higher in the horizontal plane than in the vertical.

Image **9370_8** (1700× magnification), at double the magnification of the previous image, is a good view of shale fabric and the siltiness of the sample. The influence of compaction around larger clay particles is identified by the dashed line. Sites of plucked grains occur in the upper centre and upper right.

An EDX analysis of a number of particles in image **9370_9** indicates the presence of quartz, sodium feldspar, pyrite and perhaps detrital clay. The particle identified as detrital clay appears to be a clay sheet turned upright that is in situ.

As the clay sheets compress around a particle, porosity may be created at the edges, depending on the degree of compaction around the particle. Image 9370_6 shows this behaviour at the edges of the plucked grains, although this also may be due to core unloading. The arrow in image 9370_9 indicates an example of complete compaction around a particle.

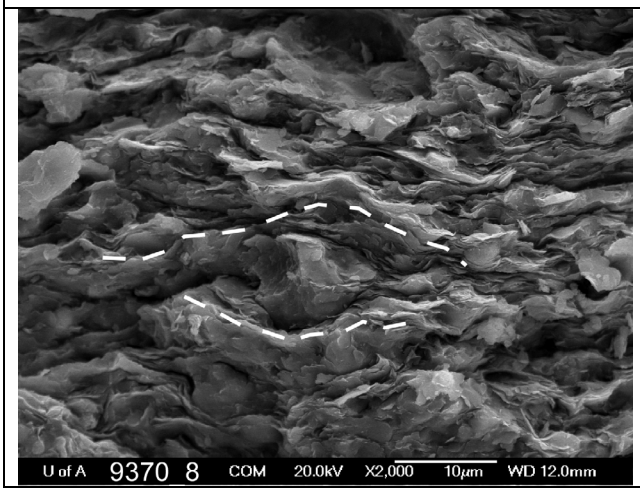

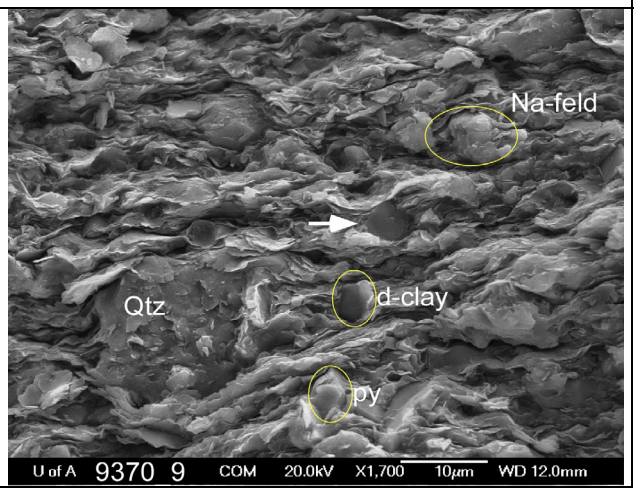

EDX results for sample 9370

Composition	Image	ID on Image
Pyritized shell fragments (9370_EDX_002)	9238_3 and 4	Yellow arrow
Illite (9370_EDX_003)	9370_6	
Potassium feldspar (9370_EDX_004)	9370_6	P-Feld
Quartz, pyrite and detrital clay (EDX not saved)	9370_9	Qtz, circle with py, circle with d-clay
Sodium feldspar (9370_EDX_005)	9370_9	Circle with Na-feld

Note: The depth of penetration of the EDX analysis is ~1–2 µm, so the chemistry below the surface may dominate the surface mineral.

Majeau Lake Formation, Sample 9386, UWI 100/10-30-053-14W5/00, 10,393.5 ft. (3167.9 m) Core Depth

The sample is massive, organic-rich and slightly friable black shale.

Image	Magnification
9386_1	25×
9386_2	100×
9386_3	250×
9386_4	1000×
9386_5	2500×
9386_6	2500×
9238_7 (backscatter)	250×
9238_8	250×
9386_9	10000×
9386_10	2500×

Image **9386_1** is a low-magnification (25×) view with bedding trending approximately east. There are three fractures traversing the sample, as indicated by the arrows, with the middle fracture exhibiting the highest dip. The texture is fairly homogeneous, with little porosity visible at this magnification. An EDX overview suggested that the main components are calcite and illite-type clay. The box identifies the location of image 9386_2.

Image **9386_2** (100× magnification) was taken in the upper middle of image 9386_1 between the two fracture surfaces identified by the upper and lower arrows. The fracture surfaces are again identified on image 9386_2. The box outlines the location of image 9386_3.

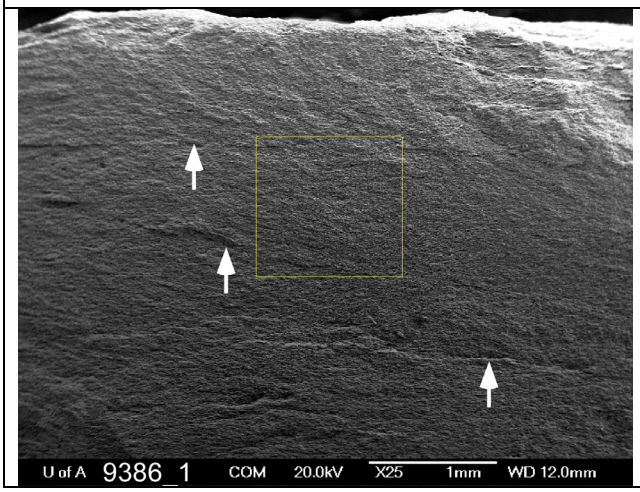

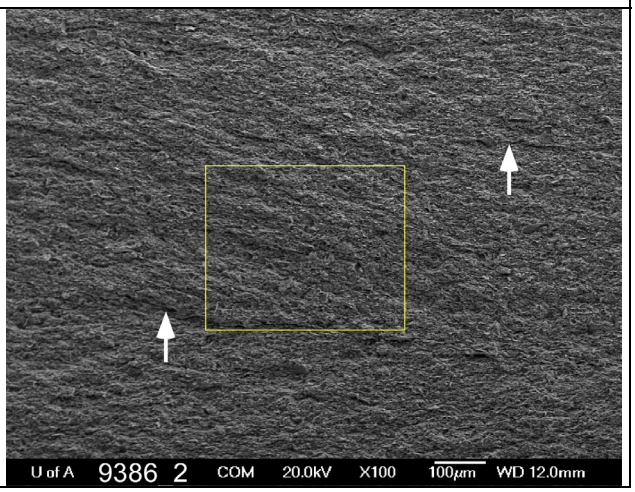

Porosity and the outline of some larger grains are visible in image **9386_3** (250× magnification). The lower fracture from image 9386_2 is visible at the bottom (identified by the lower arrow). However, as in the last image, additional fractures are visible at a higher magnification. Bedding clearly trends east-southeast. There is an occasional large pore, ~10–15 µm in diameter, but most of the pores are less than 10 µm. The red arrow identifies the general location of image 9238_4.

Image **9238_4** (1000× magnification) was taken near the lower centre of the previous image, near the 15µm grain (red arrow). Several minerals were identified by EDX analysis (not saved), including mica (muscovite), calcite, dolomite and quartz. There seems to be a reasonable amount of small diameter porosity in this view, although we cannot be certain of the amount of plucking of small (<2–4 µm) grains. The three yellow arrows indicate linear pores that were likely the sites of plucked mica grains. Most grains in this view are in the 2–4 µm range and consist of detrital and perhaps authigenic grains.

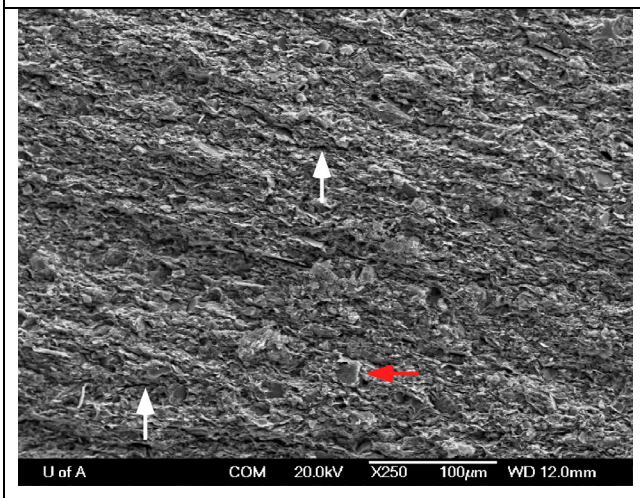

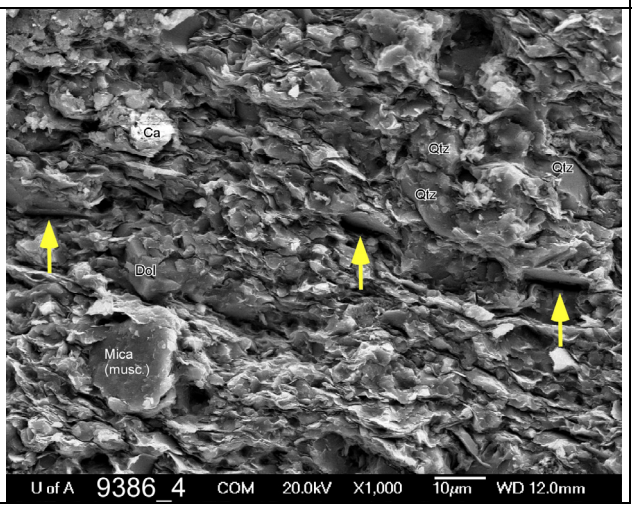

Image **9386_5** (2500× magnification) was taken near the dolomite crystal in the previous image. Porosity in this view is low and consists mainly of pores between grains and at the boundaries between clay sheets and grains.

There is a range of pore sizes and shapes in image **9386_6** (2500× magnification), but the sample has a low overall porosity dominated by small pores <1–2 µm in diameter. The sample displays many clay- and silt-sized particles that are wrapped in clay, some of which may be authigenic. The white arrows identify a few of the smaller particles. The image shows both a well-formed mica grain and a plucked mica site.

The upper portion of this image, above the mica grain, has a slightly different character than the lower portion. The upper area has fewer visible silt grains, and the absence of long sheets of clay, as at the bottom of the image, is noticeable. Sharp edges (see red arrows) may suggest the presence of clay-sized or lower silt-sized grains, but we cannot be certain of this.

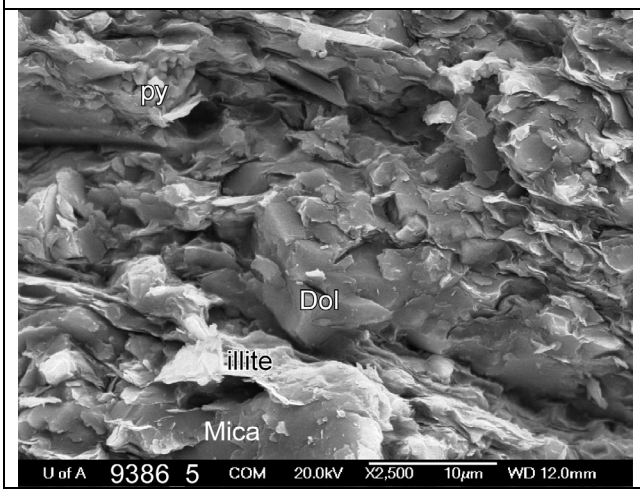

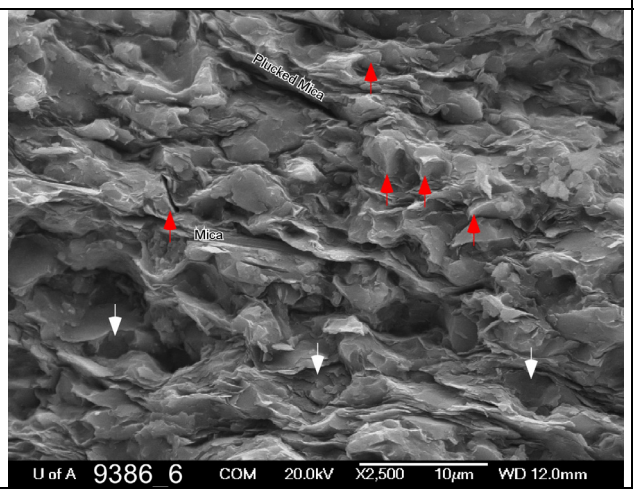

Image **9386_7** is a backscattering image of image **9386_8**. The images are relatively low magnification (250×) and reveal sporadic pyrite.

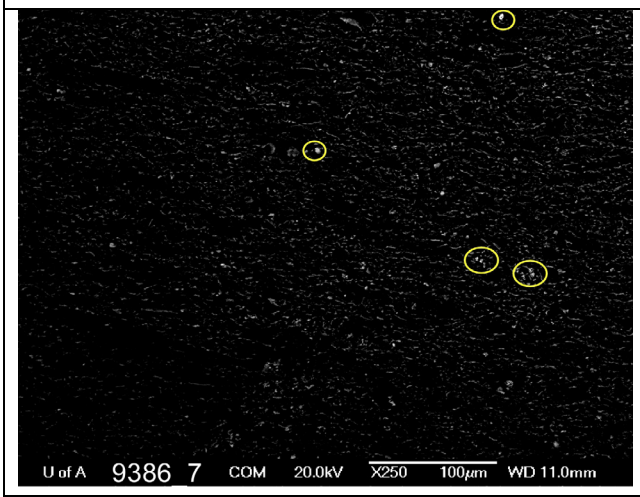

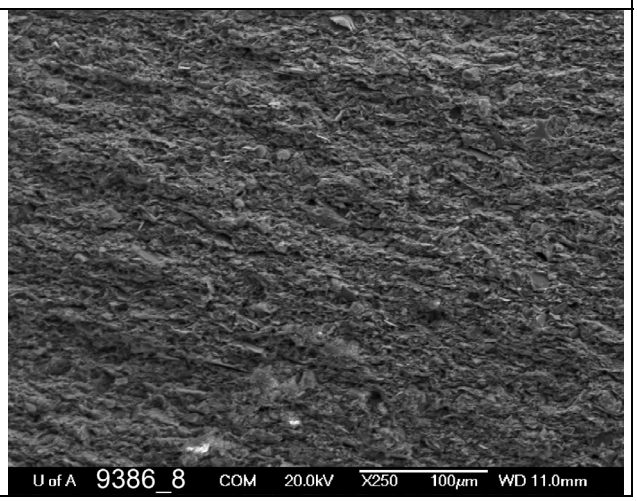

Image **9386_9** is a high-magnification (10 000×) view of porosity consisting of intergranular pores and, to a lesser degree, pores between clay domains in the middle of the image. The pores appear to be quite well connected, more so in the horizontal plane than the vertical.

An EDX analysis (not saved) on some of the particles in image **9386_10** (2500× magnification) revealed the presence of calcite, quartz, mica and pyrite in illitic clay.

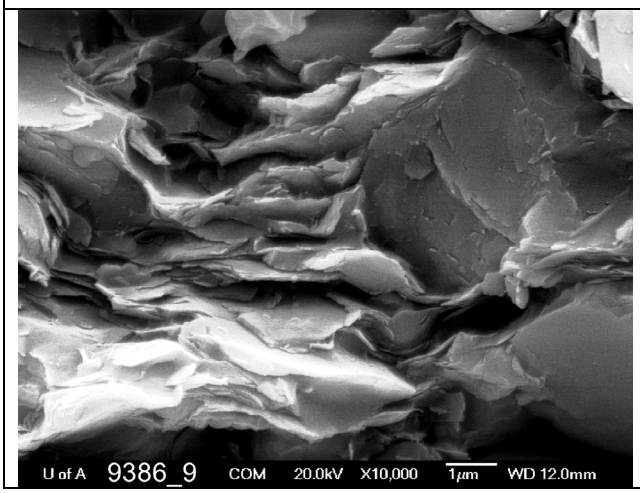

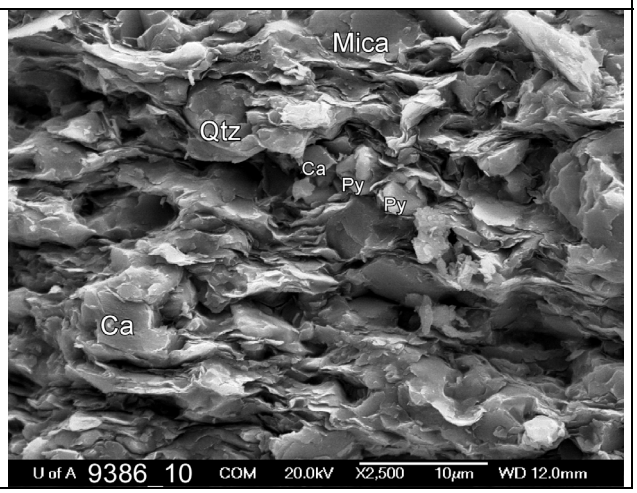

EDX results for sample 9386

Composition	Image	ID on Image
Mica (muscovite; EDX not saved)	9386_4	Mica
Calcite (EDX not saved)	9386_4	Ca
Dolomite (EDX not saved)	9386_4	Dol
Quartz (EDX not saved)	9386_4	Qtz
Calcite (EDX not saved)	9386_10	Ca
Quartz (EDX not saved)	9386_10	Qtz
Mica (EDX not saved)	9386_10	Mica
Pyrite (EDX not saved)	9386_10	Py

Note: The depth of penetration of the EDX analysis is ~1–2 μm, so the chemistry below the surface may dominate the surface mineral.

Appendix 6 – Duvernay and Muskwa Formations Mercury Porosimetry Graphs

Incremental Intrusion - Majeau Lake sample 8479

"Provides a convenient means to observe the diameter at which pore volume is concentrated" (Webb and Orr, 1997).

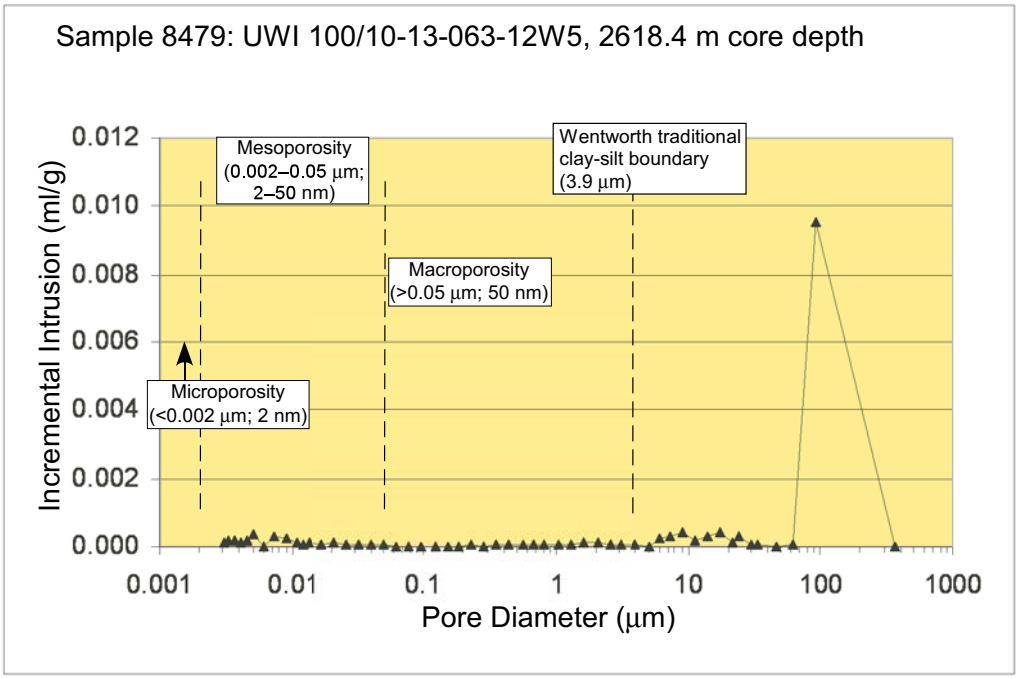

Log Differential Intrusion - Majeau Lake sample 8479

"The compression effect resulting from the use of a log scale is compensated for by dividing the specific incremental intrusion volume by the difference in logarithms of the pore diameters. This results in a curve in which equal peak areas represent equal pore volumes. This plot works best when the data points are equally spaced." (Webb and Orr, 1997).

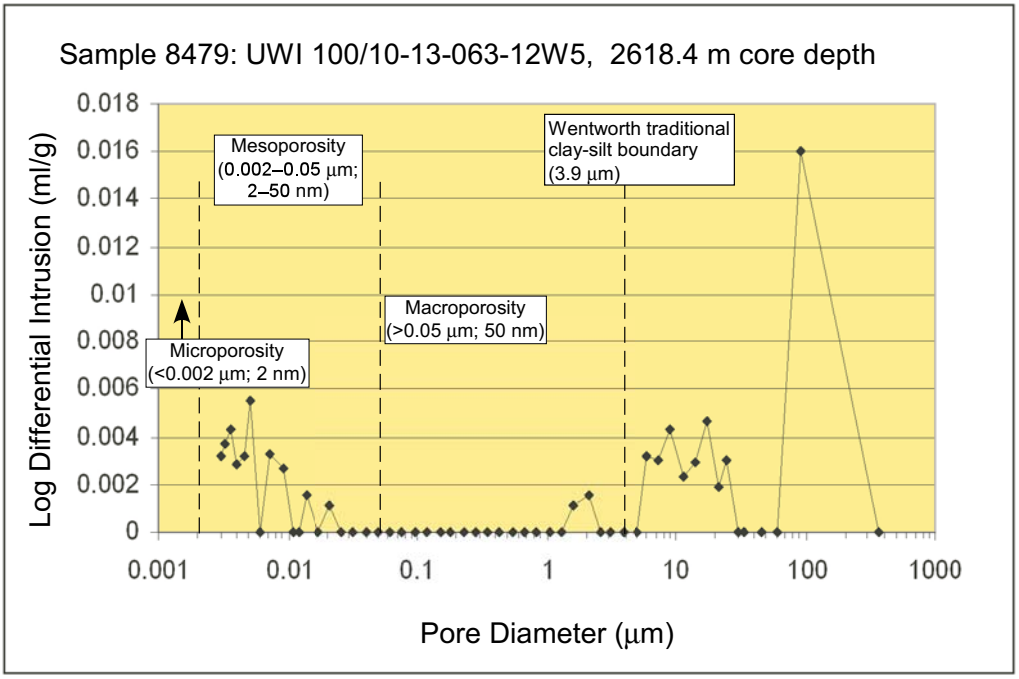

Incremental Intrusion - Muskwa sample 8995

"Provides a convenient means to observe the diameter at which pore volume is concentrated" (Webb and Orr, 1997).

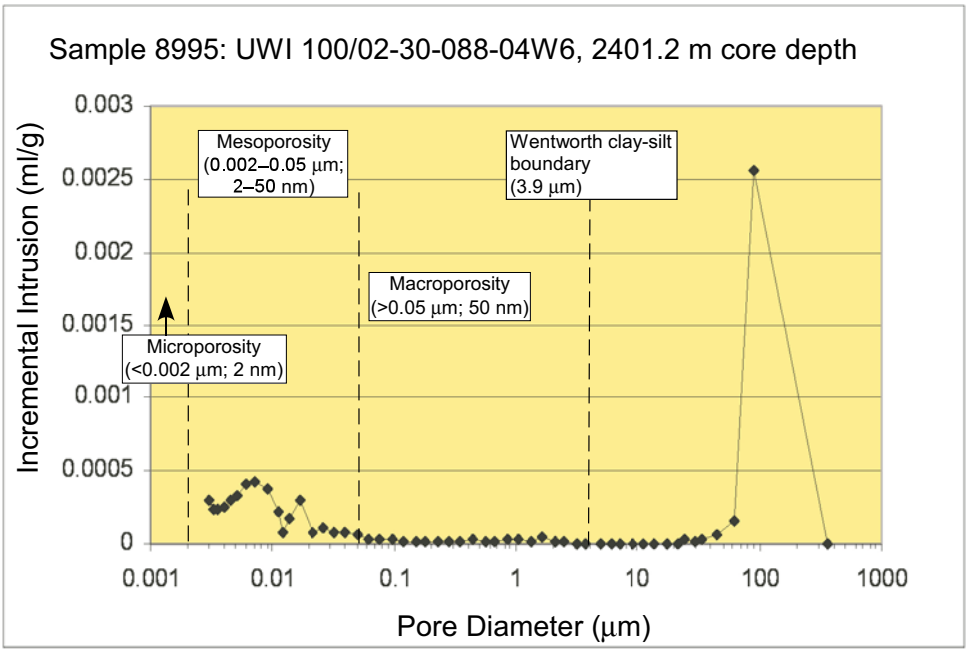

Log Differential Intrusion - Muskwa sample 8995

"The compression effect resulting from the use of a log scale is compensated for by dividing the specific incremental intrusion volume by the difference in logarithms of the pore diameters. This results in a curve in which equal peak areas represent equal pore volumes. This plot works best when the data points are equally spaced." (Webb and Orr, 1997).

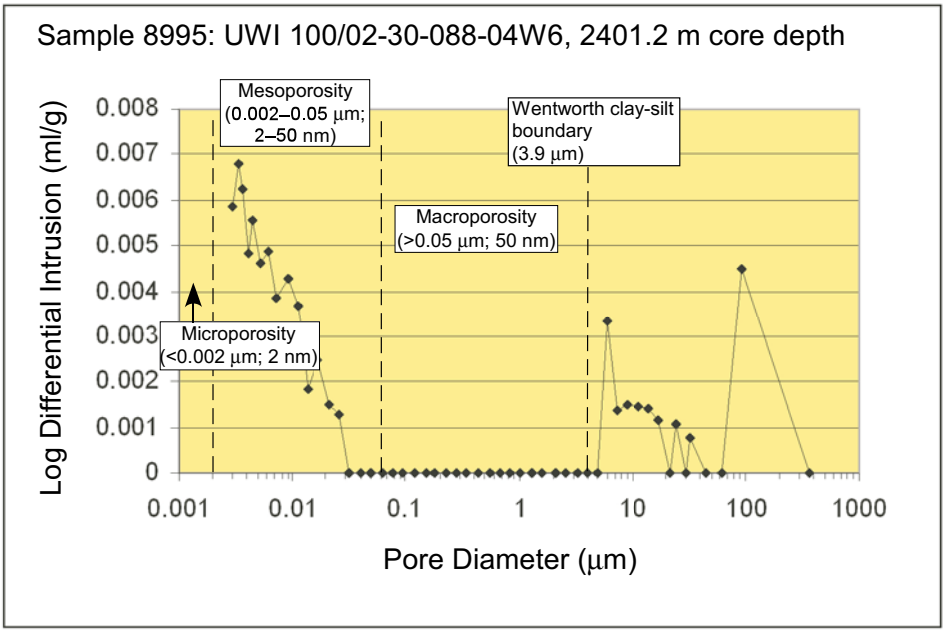

Incremental Intrusion - Muskwa sample 8995 - REPEAT

"Provides a convenient means to observe the diameter at which pore volume is concentrated" (Webb and Orr, 1997).

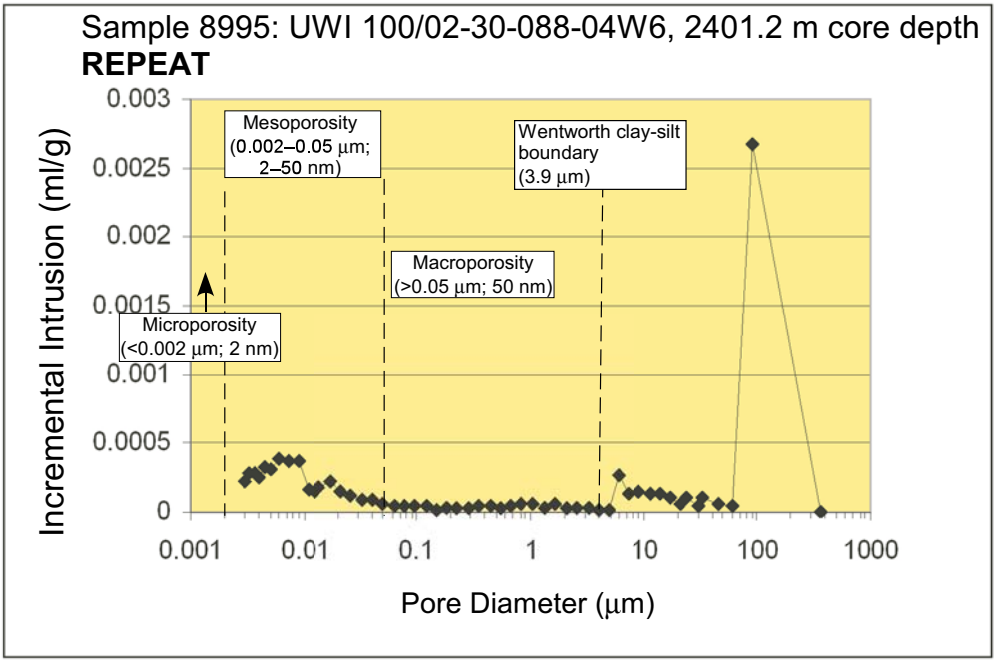

Log Differential Intrusion - Muskwa sample 8995 REPEAT

"The compression effect resulting from the use of a log scale is compensated for by dividing the specific incremental intrusion volume by the difference in logarithms of the pore diameters. This results in a curve in which equal peak areas represent equal pore volumes. This plot works best when the data points are equally spaced." (Webb and Orr, 1997).

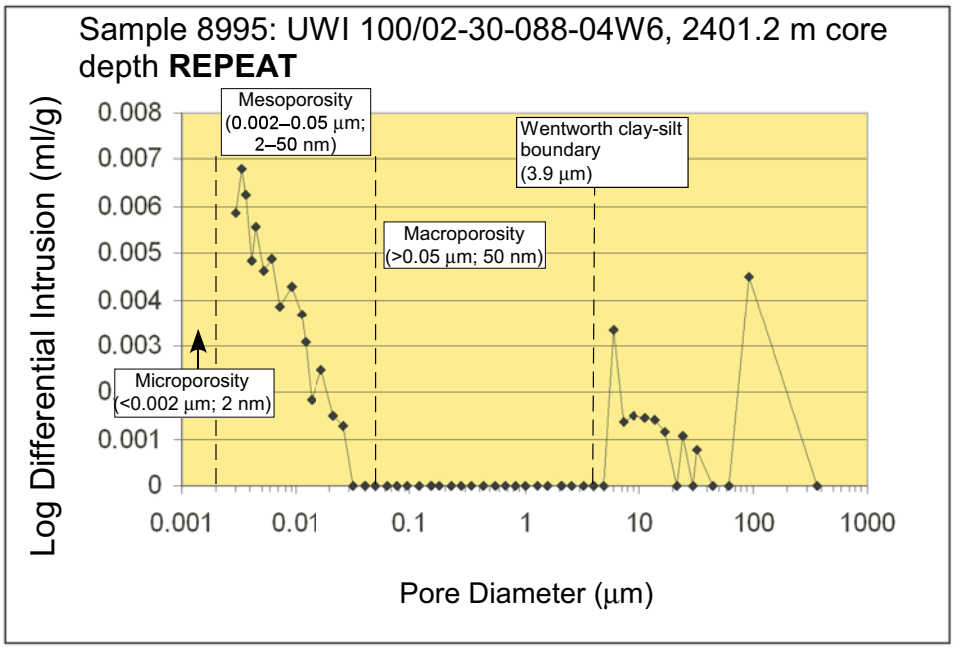

Incremental Intrusion - Duvernay sample 9238 REPEAT

"Provides a convenient means to observe the diameter at which pore volume is concentrated" (Webb and Orr, 1997).

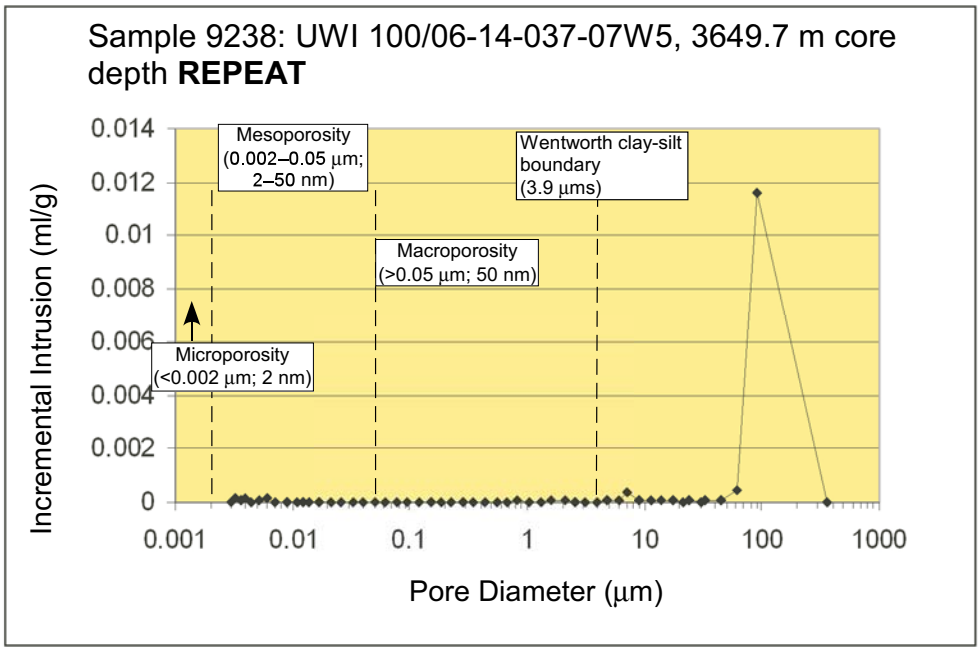

Log Differential Intrusion - Duvernay sample 9238 REPEAT

"The compression effect resulting from the use of a log scale is compensated for by dividing the specific incremental intrusion volume by the difference in logarithms of the pore diameters. This results in a curve in which equal peak areas represent equal pore volumes. This plot works best when the data points are equally spaced." (Webb and Orr, 1997).

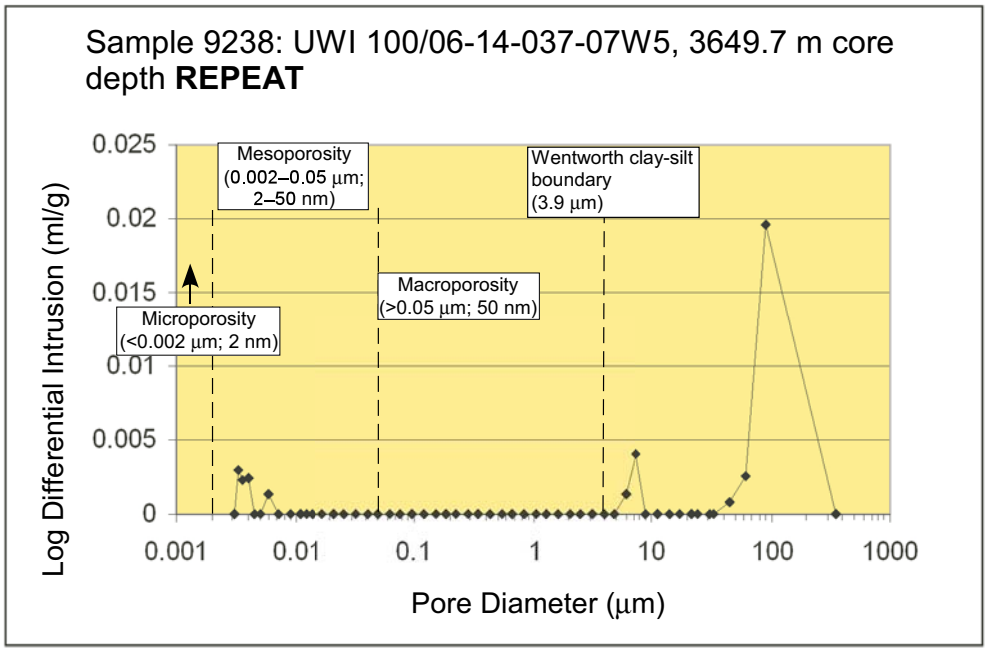

Incremental Intrusion - Muskwa sample 9370

"Provides a convenient means to observe the diameter at which pore volume is concentrated" (Webb and Orr, 1997).

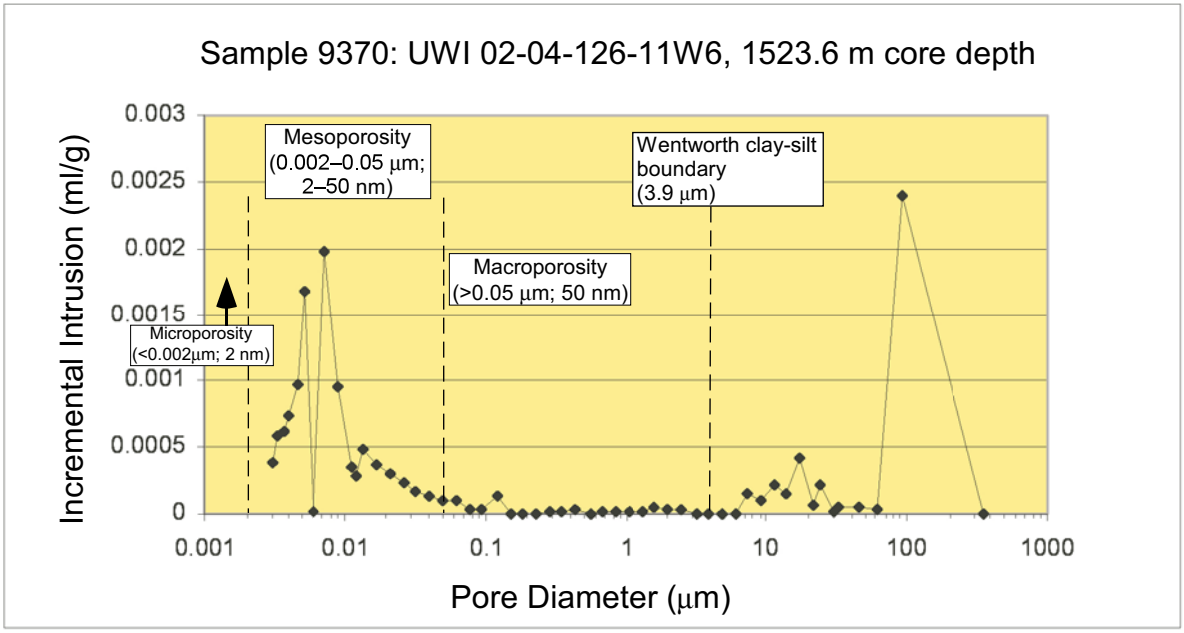

Log Differential Intrusion - Muskwa sample 9370

"The compression effect resulting from the use of a log scale is compensated for by dividing the specific incremental intrusion volume by the difference in logarithms of the pore diameters. This results in a curve in which equal peak areas represent equal pore volumes. This plot works best when the data points are equally spaced." (Webb and Orr, 1997).

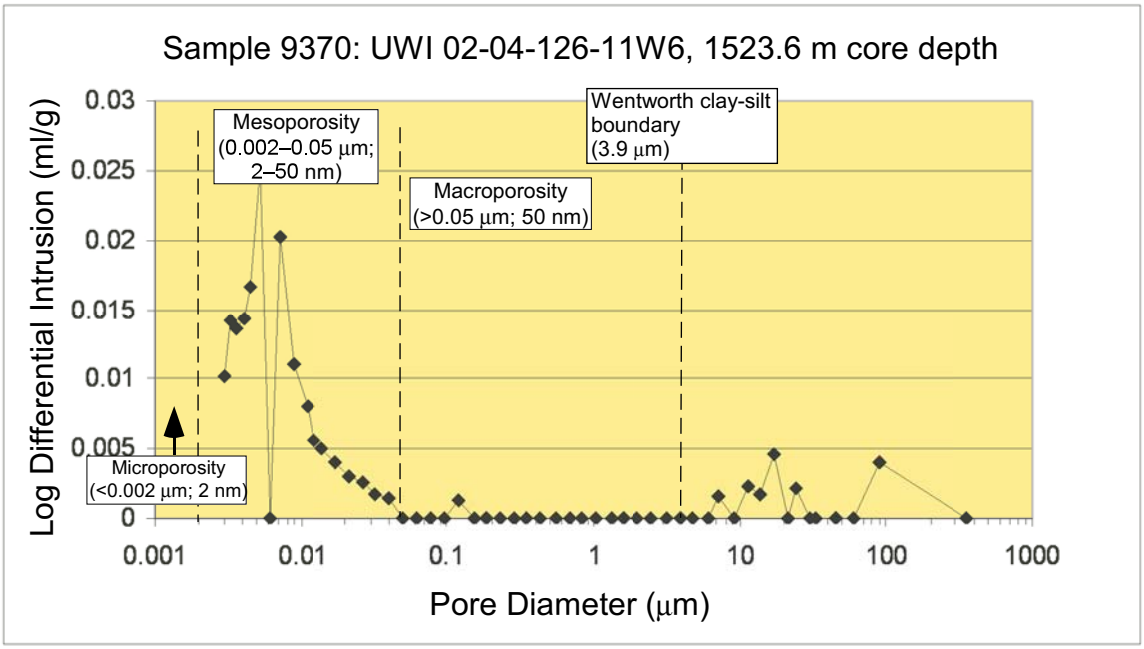

Incremental Intrusion - Muskwa sample 9370 REPEAT

"Provides a convenient means to observe the diameter at which pore volume is concentrated" (Webb and Orr, 1999).

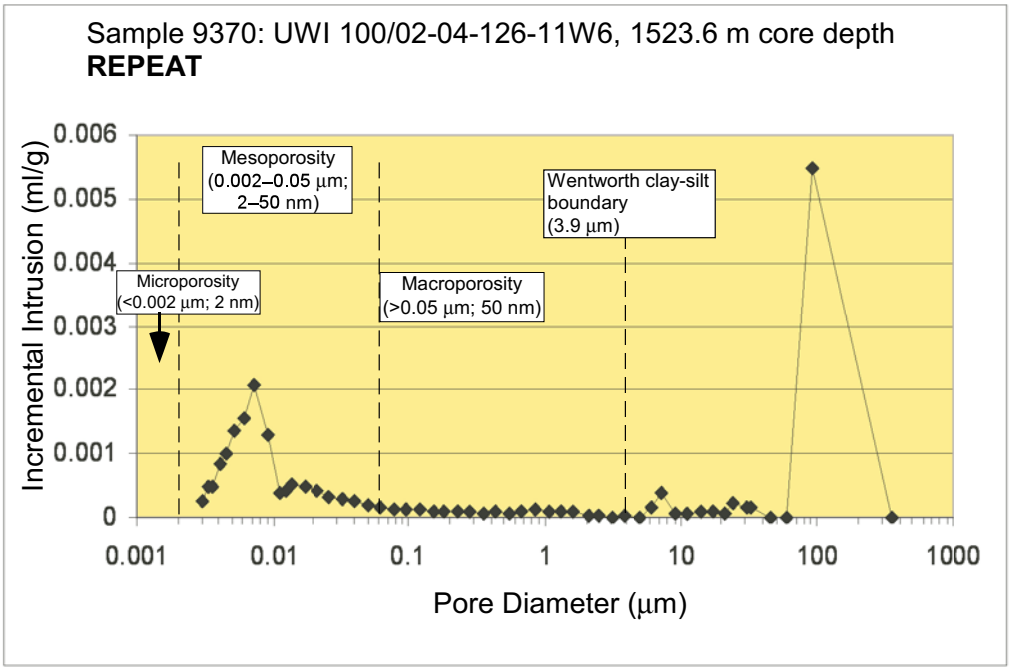

Log Differential Intrusion - Muskwa sample 9370 REPEAT

"The compression effect resulting from the use of a log scale is compensated for by dividing the specific incremental intrusion volume by the difference in logarithms of the pore diameters. This results in a curve in which equal peak areas represent equal pore volumes. This plot works best when the data points are equally spaced." (Webb and Orr, 1999).

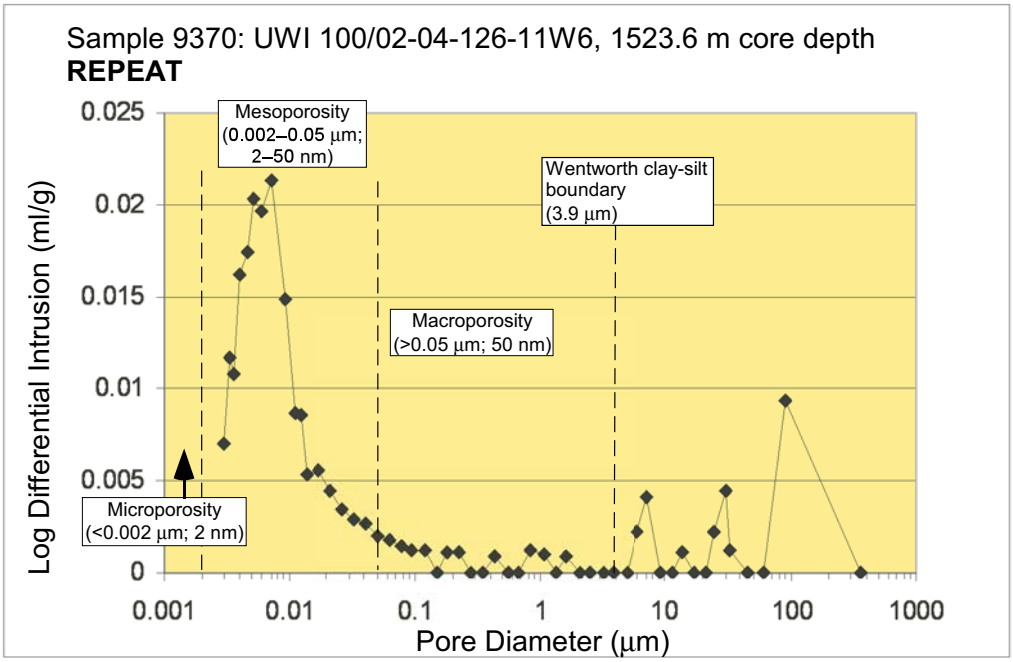

Appendix 7 – Duvernay and Muskwa Formations Permeametry

Sample No.	Depth (ft.)	Depth (m)	Ka	Kl	Comment	Approximate Angle to Bedding	Date	Probe Tip
9208	9904		0.93500	0.64800	Surface properly horizontal	Along bedding plane	25-03-09	Small
9208	9904		0.96000	0.66700	Surface properly horizontal	Along bedding plane	25-03-09	Small
9208	9904		0.55600	0.35900	Slight misalignment of sample surface (5-10°)	Along bedding plane	25-03-09	Small
9208	9904		0.55400	0.35700	Slight misalignment of sample surface (5-10°)	Along bedding plane	25-03-09	Small
9208	9904		1.11000	0.78300	Repeat measurement, surface properly horizontal	Along bedding plane	25-03-09	Small
9208	9904		1.06000	0.74600	Repeat measurement, surface properly horizontal	Along bedding plane	25-03-09	Small
9208	9904		0.01520	0.00379	Surface properly horizontal	Along bedding plane	25-03-09	Small
9208	9904		0.01490	0.00374	Surface properly horizontal	Along bedding plane	25-03-09	Small
9237		3649.1	0.03490	0.01200	Slight misalignment of sample surface (5-10°)	Along bedding plane	25-03-09	Small
9237		3649.1	0.03370	0.01140	Slight misalignment of sample surface (5-10°)	Along bedding plane	25-03-09	Small
9237		3649.1	0.02930	0.00946	Slight misalignment of sample surface (5-10°)	Along bedding plane	25-03-09	Small
9237		3649.1	0.02820	0.00899	Slight misalignment of sample surface (5-10°)	Along bedding plane	25-03-09	Small
9237		3649.1	0.05530	0.02190	Repeat measurement, surface properly horizontal	Along bedding plane	25-03-09	Small
9237		3649.1	0.05390	0.02120	Repeat measurement, surface properly horizontal	Along bedding plane	25-03-09	Small
9237		3649.1	0.05970	0.02420	Slight misalignment of sample surface (5-10°)	Along bedding plane	25-03-09	Small
9237		3649.1	0.05850	0.02360	Slight misalignment of sample surface (5-10°)	Along bedding plane	25-03-09	Small
9237		3649.1	0.02730	0.00863	Slight misalignment of sample surface (5-10°)	Along bedding plane	25-03-09	Small
9237		3649.1	0.02630	0.00817	Slight misalignment of sample surface (5-10°)	Along bedding plane	25-03-09	Small
9237		3649.1	0.01850	0.00505	Repeat measurement, surface properly horizontal	Along bedding plane	25-03-09	Small
9237		3649.1	0.01730	0.00460	Repeat measurement, surface properly horizontal	Along bedding plane	25-03-09	Small
9365	8687		0.04270	0.01560	Surface properly horizontal	Along bedding plane	25-03-09	Small
9365	8687		0.04150	0.01510	Surface properly horizontal	Along bedding plane	25-03-09	Small
9365	8687		0.04490	0.01670	Slight misalignment of sample surface (5-10°)	Along bedding plane	25-03-09	Small
9365	8687		0.04380	0.01620	Slight misalignment of sample surface (5-10°)	Along bedding plane	25-03-09	Small
9365	8687		0.08900	0.04010	Slight misalignment of sample surface (5-10°)	Along bedding plane	25-03-09	Small
9365	8687		0.08920	0.04030	Slight misalignment of sample surface (5-10°)	Along bedding plane	25-03-09	Small
9365	8687		0.07900	0.03450	Slight misalignment of sample surface (5-10°)	Along bedding plane	25-03-09	Small
9365	8687		0.07840	0.03420	Slight misalignment of sample surface (5-10°)	Along bedding plane	25-03-09	Small
9365	8687		0.08110	0.03570	Repeat measurement, surface properly horizontal	Along bedding plane	25-03-09	Small
9386	10393.5		0.54500	0.35000	Slight misalignment of sample surface (5-10°)	Along bedding plane	25-03-09	Small
9386	10393.5		0.56200	0.36300	Slight misalignment of sample surface (5-10°)	Along bedding plane	25-03-09	Small
9386	10393.5		0.39400	0.24200	Slight misalignment of sample surface (5-10°)	Along bedding plane	25-03-09	Small
9386	10393.5		0.40700	0.25100	Slight misalignment of sample surface (5-10°)	Along bedding plane	25-03-09	Small
9386	10393.5		0.42300	0.26200	Slight misalignment of sample surface (5-10°)	Along bedding plane	25-03-09	Small
9386	10393.5		0.45800	0.28700	Slight misalignment of sample surface (5-10°)	Along bedding plane	25-03-09	Small
9386	10393.5		0.46000	0.28900	Slight misalignment of sample surface (5-10°)	Along bedding plane	25-03-09	Small
9386	10393.5		0.53800	0.34600	Repeat measurement, surface properly horizontal	Along bedding plane	25-03-09	Small
9386	10393.5		0.53900	0.34700	Repeat measurement, surface properly horizontal	Along bedding plane	25-03-09	Small
9386	10393.5		302.00000	287.00000	Sample tilted during measurement	Along bedding plane	25-03-09	Small
9386	10393.5		407.00000	388.00000	Sample tilted during measurement	Along bedding plane	25-03-09	Small

Legend

Column Label	Label Description
Sample No.	AGS sample number
Depth (ft., m)	Sample depth in original units
Ka	Permeability to air
Kl	Permeability to liquid (nitrogen)
Comment	Comment on the horizontality of the sample surface during measurement
Approximate Angle to Bedding	Measured angle of the measurement spot to bedding or observable fractures
Date	Date of analysis
Probe Tip	Probe tip size (small or large)

Note: Leak permeability tests (Kg) of probe seals (before sample analysis) yielded values of ~0.0034–0.0043 mD

Appendix 8 – Duvernay and Muskwa Formations Helium Pycnometry

Sample No.	Site No.	Run No.	Vr (cm^3)	Vc (cm^3)	P1	P2	P1/P2	(P1/P2)–1	Vs (cm^3)	Avg. Vs (cm^3)	Wt. (g)	Gdensity (g/cm^3)
8479	D21	1	88.512	147.903	17.259	6.505	2.653	1.653	1.576			
8479	D21	2	88.512	147.903	17.201	6.484	2.653	1.653	1.607			
8479	D21	3	88.512	147.903	17.311	6.526	2.653	1.653	1.626	1.603	4.160	2.595
8493	D7	1	88.512	147.903	17.292	6.522	2.651	1.651	1.740			
8493	D7	2	88.512	147.903	17.277	6.517	2.651	1.651	1.764			
8493	D7	3	88.512	147.903	17.255	6.509	2.651	1.651	1.775	1.760	4.600	2.614
8995	D31	1	88.512	147.903	17.238	6.500	2.652	1.652	1.681			
8995	D31	2	88.512	147.903	17.012	6.413	2.653	1.653	1.616			
8995	D31	3	88.512	147.903	17.249	6.501	2.653	1.653	1.568	1.622	4.150	2.559
9208	D10	1	88.512	147.903	17.235	6.489	2.656	1.656	1.324			
9208	D10	2	88.512	147.903	17.374	6.543	2.655	1.655	1.384			
9208	D10	3	88.512	147.903	17.257	6.499	2.655	1.655	1.386	1.365	3.550	2.601
9228	D22	1	88.512	147.903	17.325	6.519	2.658	1.658	1.184			
9228	D22	2	88.512	147.903	17.213	6.478	2.657	1.657	1.226			
9228	D22	3	88.512	147.903	17.255	6.494	2.657	1.657	1.233	1.214	2.980	2.455
9238	D1	1	88.512	147.903	17.267	6.534	2.643	1.643	2.510			
9238	D1	2	88.512	147.903	17.287	6.541	2.643	1.643	2.489			
9238	D1	3	88.512	147.903	17.351	6.566	2.643	1.643	2.517	2.506	6.110	2.439
9365	D6	1	88.512	147.903	17.257	6.485	2.661	1.661	0.879			
9365	D6	2	88.512	147.903	17.278	6.494	2.661	1.661	0.919			
9365	D6	3	88.512	147.903	17.283	6.495	2.661	1.661	0.887	0.895	2.180	2.436
9370	D34	1	88.512	147.903	17.342	6.531	2.655	1.655	1.386			
9370	D34	2	88.512	147.903	17.301	6.516	2.655	1.655	1.402			
9370	D34	3	88.512	147.903	17.287	6.512	2.655	1.655	1.448	1.412	3.460	2.451
9386	D11	1	88.512	147.903	17.283	6.508	2.656	1.656	1.358			
9386	D11	2	88.512	147.903	17.270	6.504	2.655	1.655	1.390			
9386	D11	3	88.512	147.903	17.211	6.481	2.656	1.656	1.362	1.370	3.520	2.570

Legend

Column Label	Label Description
Sample No.	AGS sample number
Site No.	Site location number
Run No.	Number of times each sample was tested
Vr	Reference volume = 88.512 cm^3
Vc	Volume of sample cell = 147.903 cm^3
P1	Pressure (psi) after pressurizing the reference volume
P2	Pressure (psi) after including Vc
Vs	Volume of the solid
Avg. Vs	Average volume of the solid
Wt.	Weight of the sample
Gdensity	Grain density